ATG16L1 in myeloid cells limits colorectal tumor growth in Apc Min/+ mice infected with colibactin-producing Escherichia coli via decreasing inflammasome activation

Laurène Salesse, Angéline Duval, Pierre Sauvanet, Alison da Silva, Nicolas Barnich, Catherine Godfraind, Guillaume Dalmasso, Hang Thi Thu Nguyen

Autophagy

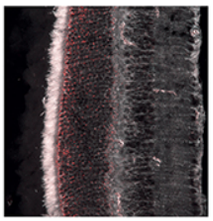

Autophagy

ISSN: (Print) (Online) Journal homepage: www.tandfonline.com/journals/kaup20

ATG16L1 in myeloid cells limits colorectal tumor growth in *Apc*$^{Min/+}$ mice infected with colibactin-producing *Escherichia coli* via decreasing inflammasome activation

Laurène Salesse, Angéline Duval, Pierre Sauvanet, Alison Da Silva, Nicolas Barnich, Catherine Godfraind, Guillaume Dalmasso & Hang Thi Thu Nguyen

To cite this article: Laurène Salesse, Angéline Duval, Pierre Sauvanet, Alison Da Silva, Nicolas Barnich, Catherine Godfraind, Guillaume Dalmasso & Hang Thi Thu Nguyen (10 Jun 2024): ATG16L1 in myeloid cells limits colorectal tumor growth in *Apc*$^{Min/+}$ mice infected with colibactin-producing *Escherichia coli* via decreasing inflammasome activation, Autophagy, DOI: 10.1080/15548627.2024.2359770

To link to this article: https://doi.org/10.1080/15548627.2024.2359770

AUTOPHAGY
https://doi.org/10.1080/15548627.2024.2359770

Taylor & Francis
Taylor & Francis Group

RESEARCH PAPER

OPEN ACCESS Check for updates

ATG16L1 in myeloid cells limits colorectal tumor growth in *Apc*$^{Min/+}$ mice infected with colibactin-producing *Escherichia coli* via decreasing inflammasome activation

Laurène Salesse[a], Angéline Duval[a], Pierre Sauvanet[a,b], Alison Da Silva[a], Nicolas Barnich[a], Catherine Godfraind[a,c], Guillaume Dalmasso[a], and Hang Thi Thu Nguyen[a]

[a]M2iSH, UMR 1071 Inserm, University of Clermont Auvergne, INRAE USC 1382, CRNH, Clermont-Ferrand, France; [b]Department of Digestive and Hepatobiliary Surgery, CHU, Clermont-Ferrand, France; [c]Department of Pathology, CHU Gabriel Montpied, Clermont-Ferrand, France

ABSTRACT

Escherichia coli strains producing the genotoxin colibactin, designated as CoPEC (colibactin-producing *E. coli*), have emerged as an important player in the etiology of colorectal cancer (CRC). Here, we investigated the role of macroautophagy/autophagy in myeloid cells, an important component of the tumor microenvironment, in the tumorigenesis of a susceptible mouse model infected with CoPEC. For that, a preclinical mouse model of CRC, the *Apc*$^{Min/+}$ mice, with *Atg16l1* deficiency specifically in myeloid cells (*Apc*$^{Min/+}$/*Atg16l1[ΔMC]*) and the corresponding control mice (*Apc*$^{Min/+}$), were infected with a clinical CoPEC strain 11G5 or its isogenic mutant 11G5Δ*clbQ* that does not produce colibactin. We showed that myeloid cell-specific *Atg16l1* deficiency led to an increase in the volume of colonic tumors in *Apc*$^{Min/+}$ mice under infection with 11G5, but not with 11G5Δ*clbQ*. This was accompanied by increased colonocyte proliferation, enhanced inflammasome activation and IL1B/IL-1β secretion, increased neutrophil number and decreased total T cell and cytotoxic CD8$^+$ T cell numbers in the colonic mucosa and tumors. In bone marrow-derived macrophages (BMDMs), compared to uninfected and 11G5Δ*clbQ*-infected conditions, 11G5 infection increased inflammasome activation and IL1B secretion, and this was further enhanced by autophagy deficiency. These data indicate that ATG16L1 in myeloid cells was necessary to inhibit colonic tumor growth in CoPEC-infected *Apc*$^{Min/+}$ mice *via* inhibiting colibactin-induced inflammasome activation and modulating immune cell response in the tumor microenvironment.

Abbreviation: AOM, azoxymethane; APC, APC regulator of WNT signaling pathway; ATG, autophagy related; *Atg16l1[ΔMC]* mice, mice deficient for *Atg16l1* specifically in myeloid cells; CASP1, caspase 1; BMDM, bone marrow-derived macrophage; CFU, colony-forming unit; CoPEC, colibactin-producing *Escherichia coli*; CRC, colorectal cancer; CXCL1/KC, C-X-C motif chemokine ligand 1; ELISA, enzyme-linked immunosorbent assay; IL, interleukin; MC, myeloid cell; MOI, multiplicity of infection; PBS, phosphate-buffered saline; *pks*, polyketide synthase; qRT-PCR, quantitative real-time reverse-transcription polymerase chain reaction; siRNA, small interfering RNA; TME, tumor microenvironment; TNF/TNF-α, tumor necrosis factor.

ARTICLE HISTORY
Received 6 November 2023
Revised 12 May 2024
Accepted 21 May 2024

KEYWORDS
Autophagy; bacterial infection; colibactin-producing *E. coli*; colorectal cancer; toxin

Introduction

Colorectal cancer (CRC) is the third most common cancer and the second leading cause of mortality by cancer worldwide [1]. The etiology of CRC is highly complex and involves both genetic and environmental factors [2]. Indeed, only a small proportion of CRC are genetically predisposed, and approximately 70–90% of CRC are sporadic or non-inherited. Environmental factors, such as western dietary habits, physical inactivity, smoking, and heavy alcohol consumption have been identified as risk factors for sporadic CRC. Some diseases including obesity, diabetes type 2 and inflammatory bowel diseases have been also associated with increased risk to develop CRC [1].

Intestinal microbiota has emerged as an important player in CRC etiology [2]. Advances in microbiome profiling have revealed gut dysbiosis in CRC patients compared to healthy controls. In particular, putatively pro-carcinogenic bacteria, including *Fusobacterium nucleatum*, *Escherichia coli*, *Bacteroides fragilis*, *Enterococcus faecalis*, *Streptococcus gallolyticus* and *Peptostreptococcus spp*., have been detected in CRC tumors with a higher abundance, whereas those with potentially protective properties, including *Roseburia*, *Clostridium*, *Faecalibacterium* and *Bifidobacterium*, are reduced [3].

In particular, *Escherichia coli* strains harboring the polyketide synthase (*pks*) pathogenicity island, which encodes the genotoxin colibactin, have been shown to be more prevalent in the biopsies of CRC patients compared to control patients [4–7]. CoPEC have been shown to induce deleterious effects in eukaryotic cells, including DNA double-strand breaks, chromosomic instability, cell cycle arrest and a senescence-associated secretory phenotype, thus promoting proliferation of adjacent uninfected cells *via* inflammatory mediators and growth factors [2]. Importantly, a direct link between a distinct mutational signature caused by exposure of human intestinal epithelial cells to CoPEC and known CRC driver mutations was shown [8].

CONTACT Hang Thi Thu Nguyen hang.nguyen@uca.fr M2iSH, UMR 1071 Inserm, University of Clermont Auvergne, INRAE USC 1382, CRNH, 28 Place Henri Dunant Clermont-Ferrand 63000, France

Supplemental data for this article can be accessed online at https://doi.org/10.1080/15548627.2024.2359770

We recently showed that autophagy is a key mechanism of host defense to CoPEC infection [9]. Autophagy is an evolutionarily conserved intracellular process that involves the sequestration of dangerous cytosolic components or invading pathogens into a double-membrane vesicle called autophagosome, which subsequently fuses with lysosome to deliver its cargo for degradation [10–12]. Autophagy plays a pivotal role in the regulation of intestinal homeostasis, gut ecology, intestinal immune responses and anti-microbial protection [10]. We showed that autophagy in intestinal epithelial cells is necessary to inhibit the genotoxic and protumoral properties of CoPEC, limiting the number and the volume of colorectal tumors in a susceptible mouse model of CRC, the $Apc^{Min/+}$ mice, infected with CoPEC [9]. We also showed that CoPEC induce the formation of invasive carcinomas in a mouse model lacking genetic susceptibility or the use of a carcinogen, and the CoPEC-induced tumorigenesis is further increased by intestinal epithelial cell-specific autophagy deficiency [13]. Mechanistically, the carcinogenic effect of CoPEC is mediated *via* the induction of DNA damage, and autophagy in intestinal epithelial cells is necessary to inhibit this [13]. This, in turn, could lead to genetic mutations that are required for CRC initiation. These works importantly highlight the role of CoPEC as a driver of CRC development, and the importance of autophagy in intestinal epithelial cells in inhibiting the carcinogenic properties of CoPEC.

The tumor microenvironment (TME) plays a critical role in cancer development and progression. Indeed, the complex interplay between cancer cells and the immune components of the TME has been extensively investigated in the past few decades. Tumor-infiltrating immune cells including myeloid-derived suppressor cells/MDSC, tumor-associated macrophages, and cytotoxic lymphocytes are critical determinants of cancer outcomes [14]. Recently, it was shown that colonization of CRC patients with CoPEC is associated with a decrease of tumor-infiltrating T lymphocytes [15]. Furthermore, CoPEC infection decreases total T cell and cytotoxic $CD8^+$ T cell numbers in the colonic mucosa of $Apc^{Min/+}$ mice [15]. Given the well described anti-tumoral function of cytotoxic $CD8^+$ T cells [16], this study indicates that CoPEC could promote a pro-carcinogenic immune environment through impairment of anti-tumoral T cell response.

Autophagy in myeloid cells (MCs) has been shown to be crucial in orchestrating mucosal immune responses. In particular, in these cells, autophagy has been shown to play an important role in intracellular bacterial killing and in regulating inflammasome activation, influencing the secretion of the inflammasome-associated cytokines [10]. Yet, the contribution of autophagy in MCs to colorectal carcinogenesis in the context of CoPEC infection remains uninvestigated. Here, we explored the role of autophagy in MCs in colorectal tumorigenesis under uninfected and CoPEC-infected conditions using $Apc^{Min/+}$ mice having deficiency of the autophagy-related gene *Atg16l1* in MCs.

Results

MC-specific Atg16l1 deficiency increased colonic tumor volume in $Apc^{Min/+}$ mice infected with the CoPEC 11G5 strain

As autophagy is a key regulator of immune responses, we investigated whether autophagy in MCs, an important component of the TME, has a role in colorectal carcinogenesis under CoPEC-infected condition using a preclinical mouse model of CRC. For this, we generated $Apc^{Min/+}$/*Atg16l1 [ΔMC]* mice, which have MC-specific *Atg16l1* deficiency, and their control littermates ($Apc^{Min/+}$/$Atg16l1^{flox/flox}$, hereafter termed $Apc^{Min/+}$ mice). These mice were orally administered with the clinical CoPEC 11G5 strain, or the isogenic mutant 11G5*ΔclbQ* that does not produce colibactin, or PBS alone (uninfected).

As shown in Figure 1A, mice started to lose weight from day 44 to 50 post-treatment. 11G5-infected $Apc^{Min/+}$ mice lost more body weight compared to uninfected or 11G5*ΔclbQ*-infected $Apc^{Min/+}$ mice. No significant difference in body weight was observed between the 11G5-infected $Apc^{Min/+}$ and 11G5-infected $Apc^{Min/+}$/*Atg16l1 [ΔMC]* mice (Figure 1A). Furthermore, we examined the impact of MC-specific *Atg16l1* deficiency on the bacterial colonization in the gastrointestinal tract. No significant difference in the number of 11G5 or 11G5*ΔclbQ* bacteria in the feces between $Apc^{Min/+}$/*Atg16l1[ΔMC]* and $Apc^{Min/+}$ mice was observed at different days post-infection (Figure S1A). The number of 11G5 or 11G5*ΔclbQ* bacteria associated with the colon of $Apc^{Min/+}$ and $Apc^{Min/+}$/*Atg16l1 [ΔMC]* mice, determined at the day of sacrifice, was similar (Figure S1B). This suggested that MC-specific autophagy deficiency did not influence CoPEC colonization in the colon.

The representative photos of the mouse colons taken at the day of sacrifice were shown in Figure 1B. Histological examination showed that all the polyps detected by a binocular loupe are adenocarcinomas. Infection with 11G5, but not 11G5*ΔclbQ*, led to increases in the number and volume of colonic tumors in $Apc^{Min/+}$ mice (Figure 1C, D). This was consistent with our previous publication [9]. Under 11G5-infected condition, no difference in the tumor number was observed between $Apc^{Min/+}$/*Atg16l1[ΔMC]* and $Apc^{Min/+}$ mice (Figure 1C). However, the tumor volume was increased in 11G5-infected $Apc^{Min/+}$/*Atg16l1[ΔMC]* *vs* 11G5-infected $Apc^{Min/+}$ mice (Figure 1D). Under uninfected or 11G5*ΔclbQ*-infected condition, the number and the volume of colonic tumors were not different between $Apc^{Min/+}$/*Atg16l1[ΔMC]* and $Apc^{Min/+}$ mice (Figure 1C, D). Importantly, histological scoring of the colonic sections of these mice showed an increase in 11G5-infected $Apc^{Min/+}$/*Atg16l1[ΔMC]* *vs* 11G5-infected $Apc^{Min/+}$ mice, and this was not observed under 11G5*ΔclbQ*-infected condition (Figure 1E). Representative photos of H&E-stained mouse colonic sections were shown in Figure 2.

MC-specific Atg16l1 deficiency increased colonic cell proliferation in 11G5-infected $Apc^{Min/+}$ mice

As MC-specific autophagy deficiency led to increased colonic tumor volume in 11G5-infected $Apc^{Min/+}$ mice, we sought to investigate its effect on colonic epithelial cell proliferation. qRT-PCR analysis showed that mRNA expression level of *Ccnd1/cyclin D1*, which is involved in cell cycle progression, in the colonic mucosa was not different between uninfected $Apc^{Min/+}$/*Atg16l1[ΔMC]* and $Apc^{Min/+}$ mice (Figure 3A). Infection with 11G5 increased *Ccnd1* mRNA expression in

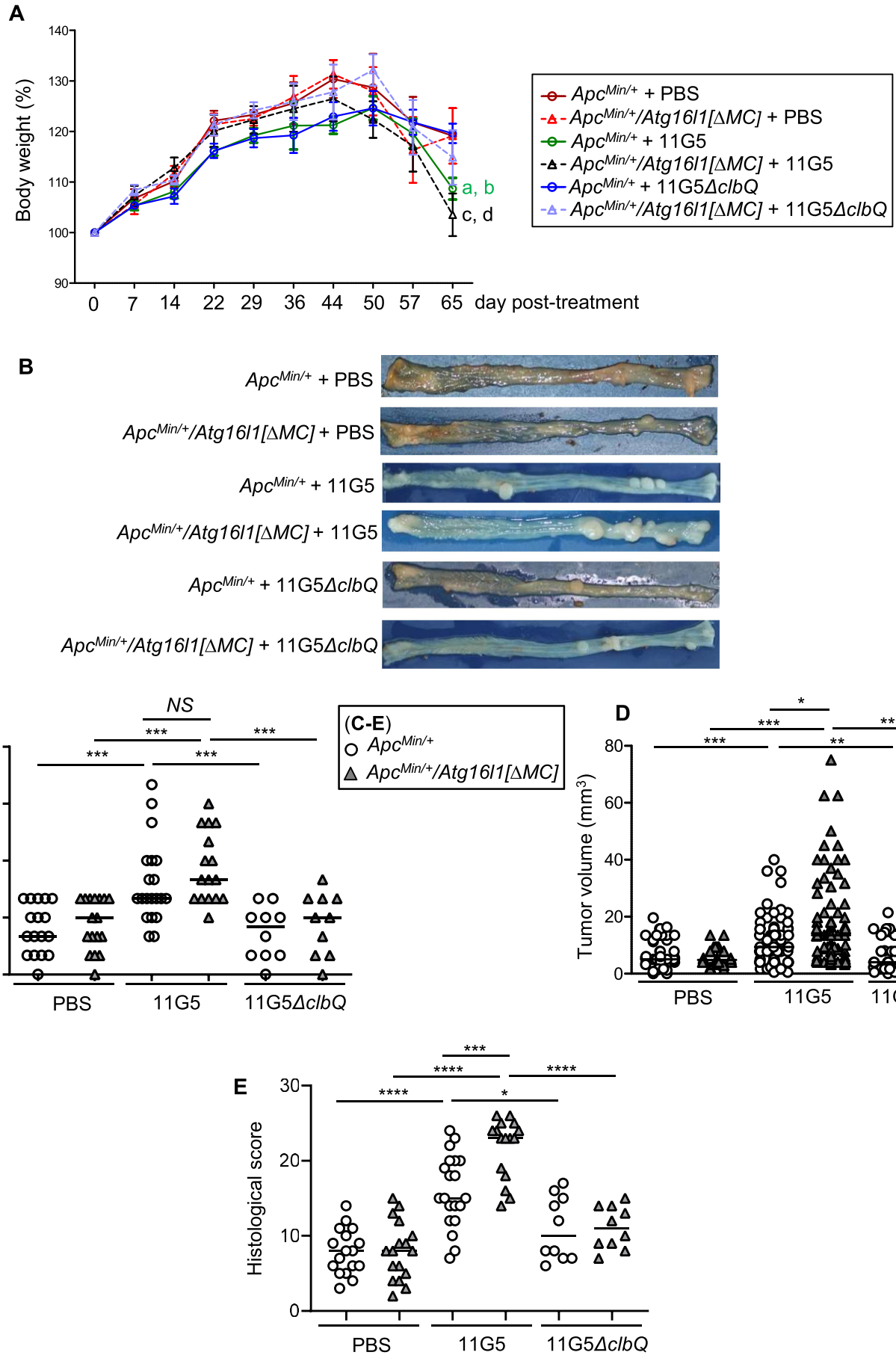

Figure 1. MC-specific *Atg16l1* deficiency led to increased colonic tumor volume in $Apc^{Min/+}$ mice infected with the CoPEC 11G5 strain. $Apc^{Min/+}$/*Atg16l1[ΔMC]* and control ($Apc^{Min/+}$/$Atg16l1^{flox/flox}$ or $Apc^{Min/+}$) mice were treated with streptomycin for 3 days, then received H_2O for 24 h. The mice were orally administered (day 0)

the colonic mucosa of $Apc^{Min/+}$ mice (Figure 3A), which was in agreement with our previous publication [9]. Interestingly, *Ccnd1* mRNA expression was increased in 11G5-infected $Apc^{Min/+}$*/Atg16l1[ΔMC] vs* 11G5-infected $Apc^{Min/+}$ mice (Figure 3A). This was not observed under 11G5*ΔclbQ*-infected condition.

These results were confirmed by immunohistochemical staining of MKI67/Ki67, a marker of cell proliferation. The number of MKI67-positive cells in the non-tumoral colonic mucosa was not different between $Apc^{Min/+}$*/Atg16l1[ΔMC]* and $Apc^{Min/+}$ mice under uninfected or 11G5*ΔclbQ*-infected conditions (Figure 3B, C). However, upon 11G5 infection, this was increased in $Apc^{Min/+}$*/Atg16l1[ΔMC] vs* $Apc^{Min/+}$ mice (Figure 3B, C). Importantly, the proliferation of tumor cells was also increased in $Apc^{Min/+}$*/Atg16l1[ΔMC] vs* $Apc^{Min/+}$ mice upon 11G5 infection, although this was not different between uninfected or 11G5*ΔclbQ*-infected groups (Figure 3B, D).

To strengthen our conclusion on colonic cell proliferation, we performed qRT-PCR and western blot analyses to determine the mRNA (Figure S2A) and protein (Figure S2B) levels, respectively, of PCNA (proliferating cell nuclear antigen), another marker of cell proliferation. As shown in Figure S2, infection with 11G5 increased *Pcna* mRNA and PCNA protein expression in the colonic mucosa of $Apc^{Min/+}$ mice, and this was not observed under 11G5*ΔclbQ*-infected condition. Interestingly, *Pcna* mRNA and PCNA protein expression was further increased by MC-specific *Atg16l1* deficiency under infection with 11G5, but not with 11G5*ΔclbQ* (Figure S2).

Together, these results showed that MC-specific *Atg16l1* deficiency led to increased proliferation of colonic epithelial cells during 11G5 infection in $Apc^{Min/+}$ mice, which could contribute to the progression of colonic tumors.

MC-specific Atg16l1 deficiency did not affect CoPEC 11G5-induced colonic DNA damage in $Apc^{Min/+}$ mice

As we have shown that induction of DNA damage is one of the mechanisms underlying the pro-carcinogenic properties of CoPEC in CRC mouse models [9, 13], we verified whether MC-specific *Atg16l1* deficiency affected 11G5-induced colonic DNA damage in $Apc^{Min/+}$ mice. Immunohistochemical staining for γH2AX, a marker of DNA double-strand breaks, showed an increase in the number of γH2AX foci per crypt in the colonic mucosa of $Apc^{Min/+}$ mice upon 11G5 infection compared to uninfected or 11G5*ΔclbQ*-infected condition (Figure 4), which was consistent with our previous study [9]. There was no significant difference in the number of γH2AX foci per crypt between 11G5-infected $Apc^{Min/+}$*/Atg16l1[ΔMC] vs* 11G5-infected $Apc^{Min/+}$ mice (Figure 4). This result suggested that MC-specific *Atg16l1* deficiency did not affect 11G5-induced colonic DNA damage in $Apc^{Min/+}$ mice.

CoPEC infection induced autophagy in macrophages in a colibactin-independent manner

To explore the mechanism by which MC-specific *Atg16l1* deficiency led to increased tumor growth in 11G5-infected $Apc^{Min/+}$ mice, we used macrophages as an *in vitro* model as macrophages are one of the predominant tumor-infiltrating immune cells supporting key processes in tumor progression [16].

First, we investigated whether autophagy was activated in human THP-1 macrophages after bacterial infection by analyzing the levels of LC3-I (cytosolic form) and LC3-II (phagophore- and autophagosome-associated form and a marker of autophagy induction [17]) by western blot. Infection with 11G5, or the mutant 11G5*ΔclbQ*, or the transcomplemented 11G5 led to increased LC3-II level compared to uninfected condition or infection with the commensal *E. coli* strains MG1655 or HS (Figure 5A, B). Infection with the nonpathogenic commensal *E. coli* MG1655 or HS strain also led to increased LC3-II level compared with the uninfected condition, although this was lower compared to CoPEC infection (Figure 5A, B). Induction of a degradative autophagy in CoPEC-infected cells was also analyzed by western blot of SQSTM1/p62 (sequestosome 1), a receptor protein that is degraded by functional autophagy. Figure S3 shows that infection with 11G5, or the mutant 11G5*ΔclbQ*, or the transcomplemented 11G5 led to decreased SQSTM1 protein level compared to uninfected or MG1655-infected condition. This result indicated that CoPEC infection induced a degradative autophagy in macrophages independently of colibactin.

To confirm these data, we used bone marrow-derived macrophages (BMDMs) from *Atg16l1[ΔMC]* mice, which have MC-specific *Atg16l1* deficiency, and the wild-type control $Atg16l1^{flox/flox}$ mice. Infection of BMDMs from $Atg16l1^{flox/flox}$ mice with 11G5, 11G5*ΔclbQ* or the transcomplemented 11G5 led to increased LC3-II levels compared to the uninfected or MG1655-infected condition (Figure 5C, D). As expected, LC3-II was not observed in BMDMs from *Atg16l1[ΔMC]* mice, indicating autophagy deficiency, either under uninfected or infected condition (Figure 5C, D).

Furthermore, the increase in LC3-II level induced by CoPEC infection observed in Figures 5A-D was also

with PBS or with 10^9 11G5 or 11G5*ΔclbQ* bacteria. Mice were sacrificed at day 65 post-administration. (A) Body weight determined at different time points was presented as percentage of body weight of the same mouse at day 0, defined as 100%. Data are means ± SEM. $^a p < 0.05$ *vs* $Apc^{Min/+}$ + PBS; $^b p < 0.05$ *vs* $Apc^{Min/+}$ +11G5*ΔclbQ*; $^c p < 0.05$ *vs* $Apc^{Min/+}$*/Atg16l1[ΔMC]* + PBS; $^d p < 0.05$ *vs* $Apc^{Min/+}$*/Atg16l1[ΔMC]* +11G5*ΔclbQ*. Statistical analysis was performed using two-way Anova test followed by Bonferroni post-test. (B) Representative photos of the colons taken at the day of sacrifice. The number (C) and volume (D) of colorectal tumors were determined using a binocular loupe. (E) The histological evaluation of the colonic sections was performed under blinded conditions by an expert anatomopathologist according to the criteria in Table S2. Statistical analysis was performed using one-way Anova test followed by Bonferroni post-test. $^* p < 0.05$; $^{**} p \leq 0.01$; $^{***} p \leq 0.001$; *NS*: not significant (C-E).

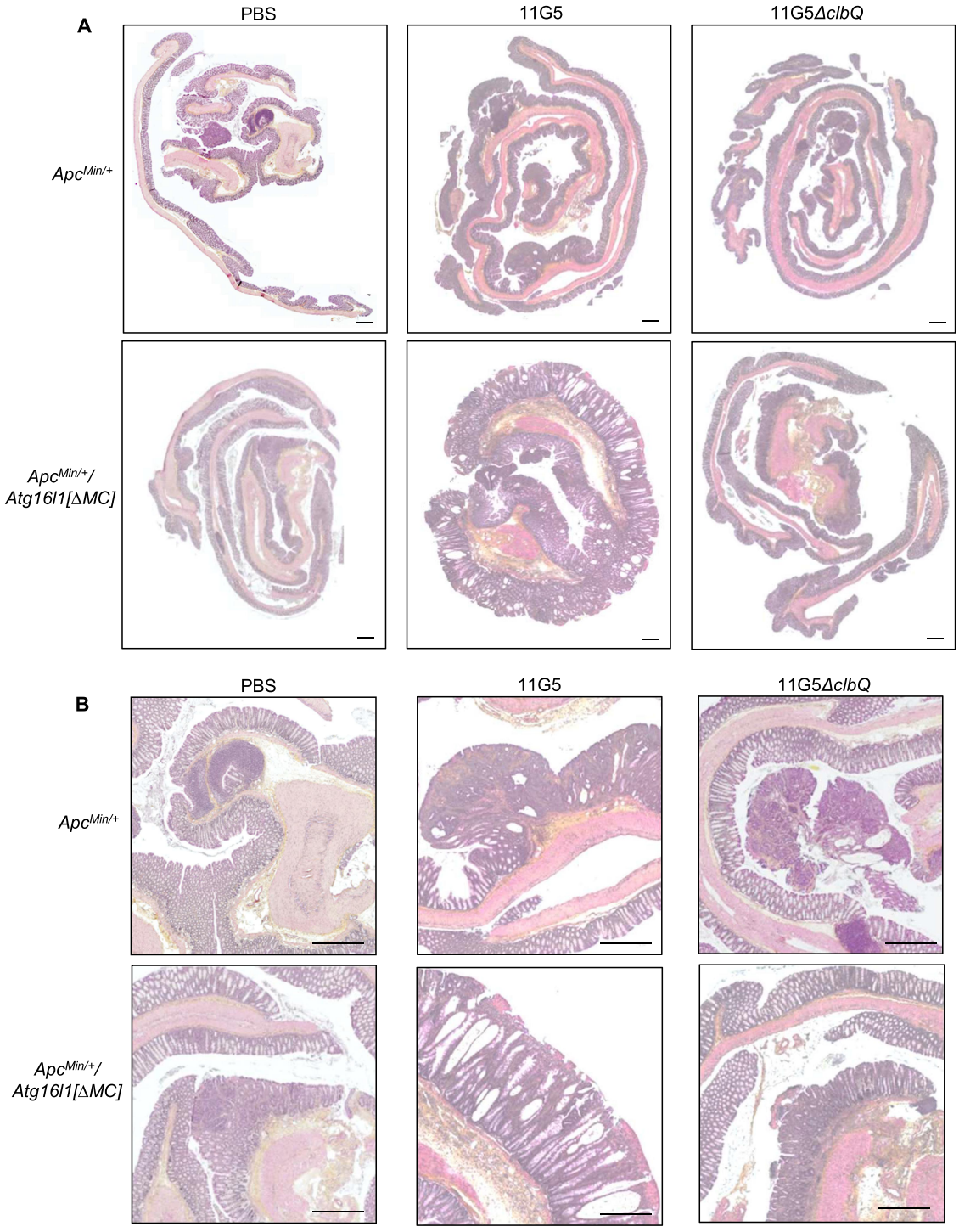

Figure 2. H&E-stained colonic sections of *Apc*$^{Min/+}$ and *Apc*$^{Min/+}$*/Atg16l1[ΔMC]* mice infected with 11G5 or 11G5*ΔclbQ* bacteria. *Apc*$^{Min/+}$*/Atg16l1[ΔMC]* and control (*Apc*$^{Min/+}$*/Atg16l1*$^{flox/flox}$ or *Apc*$^{Min/+}$) mice were treated with streptomycin for 3 days, then received H_2O for 24 h. The mice were orally administered (day 0) with PBS or with 10^9 11G5 or 11G5*ΔclbQ* bacteria. Mice were sacrificed at day 65 post-administration. Representative photos of H&E-stained mouse colonic sections at low (A) and high (B) magnifications. Bars: 500 µm.

obtained in cells treated with the inhibitor of autophagy flux bafilomycin A1 [17] (data not shown), indicating that CoPEC infection induced autophagy rather than blocked autophagy flux.

Together, these results suggested that CoPEC infection induced autophagy activation in macrophages independently of colibactin.

In an effort to show autophagy induction upon CoPEC infection *in vivo*, we performed immunofluorescent staining for LC3 using the colonic sections. As shown in Figure S4, infection with the CoPEC 11G5 strain induced an increase in LC3 accumulation, suggesting autophagy activation, in the colon of *Apc*$^{Min/+}$ mice. The autophagy induction was

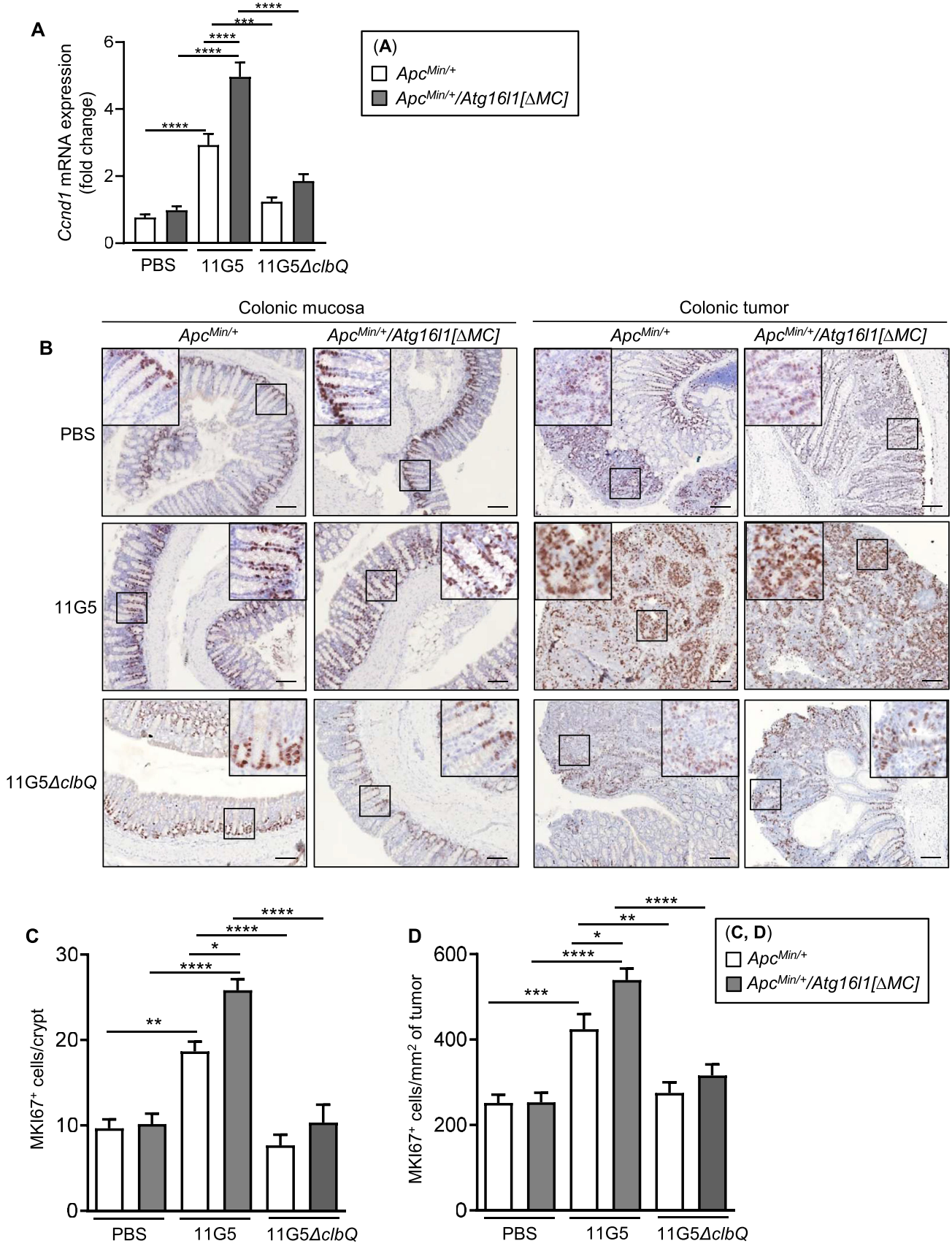

Figure 3. MC-specific *Atg16l1* deficiency led to increased colonic epithelial cell proliferation in $Apc^{Min/+}$ mice under 11G5-infected condition. $Apc^{Min/+}$/*Atg16l1[ΔMC]* and $Apc^{Min/+}$ mice were orally administered with PBS or with 10^9 11G5 or 11G5Δ*clbQ* bacteria, and sacrificed at day 65 post-administration. (A) *Ccnd1* (cyclin D1) mRNA level in the non-tumoral colonic mucosa was quantified by qRT-PCR. (B) Representative images of immunohistochemical staining for MKI67/Ki67 in the colonic mucosa and tumors. Boxes show magnified fields. Bars: 100 µm. (C) Quantification of MKI67-positive cell number/crypt determined from 40 crypts/mouse. (D) Quantification of MKI67-positive cell number/mm^2 of tumor. Values represent means ± SEM. Statistical analysis was performed using one-way Anova test followed by Bonferroni post-test. *$p < 0.05$; **$p \leq 0.01$; ***$p \leq 0.001$; ****$p \leq 0.0001$.

observed in both intestinal epithelial cells and immune cells in the *lamina propria* (Figure S4).

ATG16L1 was necessary to limit the intramacrophagic number of CoPEC

Because we have shown that autophagy is a key process to eliminate invasive *E. coli* pathobionts [13, 18–23], we sought to check the impact of *Atg16l1* deficiency on 11G5 number inside macrophages. As shown in Figure 5E, under untreated condition, the number of 11G5, 11G5Δ*clbQ* or the transcomplemented 11G5 in human THP-1 macrophages was similar and was higher than that of the nonpathogenic MG1655 strain. Treatment of THP-1 macrophages with rapamycin, an inducer of autophagy, decreased the number of intracellular 11G5, 11G5Δ*clbQ* or the transcomplemented 11G5 to similar levels (Figure 5E). Reversely, transfection of THP-1 macrophages with *ATG16L1* siRNA, which decreased markedly ATG16L1 protein level (Figure S5), led to an increase in the number of intracellular 11G5, 11G5Δ*clbQ* or the transcomplemented 11G5, compared to transfection with a control siRNA (Figure 5F).

These results were confirmed using the murine BMDMs. The number of 11G5, 11G5Δ*clbQ* or the transcomplemented 11G5 in BMDMs from *Atg16l1[ΔMC]* mice was higher than that in BMDMs from wild-type $Atg16l1^{flox/flox}$ mice (Figure 5G). No significant difference between the number of 11G5, 11G5Δ*clbQ* and the transcomplemented 11G5 was observed in both BMDMs from wild-type and *Atg16l1[ΔMC]* mice (Figure 5G).

These data suggested that autophagy was necessary to eliminate intracellular 11G5 bacteria independently of colibactin.

ATG16L1 was necessary to limit CoPEC-induced pro-inflammatory cytokine and chemokine production by macrophages

As excessive pro-inflammatory cytokine production by macrophages may lead to chronic inflammation, promoting tumorigenesis, we investigated this under CoPEC-infected condition.

Infection of BMDMs from wild-type mice with 11G5 led to an increase in the amounts of secreted pro-inflammatory cytokines IL6, IL1B and TNF/TNF-α and the chemokine CXCL1/KC, compared to uninfected or MG1655-infected condition (Figure 6A-D). Importantly, the secreted amounts of these cytokines and chemokine were higher in BMDMs from *Atg16l1[ΔMC] vs* $Atg16l1^{flox/flox}$ mice under infection with 11G5, 11G5Δ*clbQ* or the transcomplemented 11G5 (Figure 6A-D). This indicated that a functional autophagy was necessary to inhibit CoPEC-induced pro-inflammatory cytokine and chemokine production by macrophages.

For IL6, TNF and CXCL1, their secreted amounts were not different between 11G5-infected and 11G5Δ*clbQ*-infected conditions in either BMDMs from wild-type or *Atg16l1 [ΔMC]* mice (Figure 6A-C). For the secreted IL1B level, there was no significant difference between 11G5-infected and 11G5Δ*clbQ*-infected conditions in BMDMs from wild-type mice (Figure 6D). However, in BMDMs from *Atg16l1 [ΔMC]* mice, the secreted IL1B amount was increased upon infection with 11G5 or the transcomplemented 11G5 compared to 11G5Δ*clbQ* infection (Figure 6D). This indicated that in macrophages, CoPEC induced IL6, TNF and CXCL1 secretion independently of colibactin, whereas CoPEC-induced IL1B secretion was partly dependent on colibactin when *Atg16l1* is deficient.

ATG16L1 was necessary to limit CoPEC-induced inflammasome activation in macrophages dependently of colibactin

It has been shown that autophagy is required to inhibit inflammasome activation, which leads to activation of CASP1 (caspase 1) responsible to cleave pro-IL1B into mature IL1B [10]. Thus, we hypothesized that the CoPEC-induced increase in secreted IL1B amount in *Atg16l1*-deficient macrophages could be due to CoPEC-induced inflammasome activation in these cells.

(Figure 6E, F) showed that infection with 11G5, but not 11G5Δ*clbQ*, increased level of cleaved CASP1, a marker of inflammasome activation, in BMDMs from wild-type mice. CoPEC-induced cleaved CASP1 level was increased in BMDMs from *Atg16l1[ΔMC]* mice compared to wild-type mice (Figure 6E, F). These results suggested that in *Atg16l1*-deficient macrophages, 11G5 infection induced inflammasome activation, leading to increased secreted IL1B amount compared to 11G5Δ*clbQ* infection.

MC-specific Atg16l1 deficiency increased CoPEC-induced inflammasome activation and pro-inflammatory cytokine and chemokine production in the colon of $Apc^{Min/+}$ mice

To confirm the results obtained with BMDMs, we analyzed the amounts of secreted pro-inflammatory cytokines and chemokine in the non-tumoral colonic mucosa. Under uninfected condition, the amounts of secreted IL1B, IL6, TNF and CXCL1 were not significantly different between $Apc^{Min/+}$*/Atg16l1[ΔMC]* and $Apc^{Min/+}$ mice (Figure 7A-D). Under 11G5 or 11G5Δ*clbQ*-infected condition, these levels were increased in $Apc^{Min/+}$*/Atg16l1[ΔMC] vs* $Apc^{Min/+}$ mice. Infection with 11G5 or 11G5Δ*clbQ* increased the secreted amounts of IL6, TNF and CXCL1 in both $Apc^{Min/+}$ and $Apc^{Min/+}$*/Atg16l1[ΔMC]* mice with similar effect (Figure 7B-D). For the secreted IL1B amount, in $Apc^{Min/+}$ mice, this was increased under 11G5-infected or 11G5Δ*clbQ*-infected condition up to similar levels (Figure 7A). However, in $Apc^{Min/+}$*/Atg16l1[ΔMC]* mice, the secreted IL1B level was increased upon 11G5 infection *vs* 11G5Δ*clbQ* infection (Figure 7A).

To investigate the effect of CoPEC-induced inflammasome activation in the colon, we performed immunofluorescent staining for cleaved CASP1. Infection with 11G5, but not 11G5Δ*clbQ*, increased cleaved CASP1 level in both colonic mucosa (Figure 8A, C) and tumor (Figure 8B, D) from $Apc^{Min/+}$ and $Apc^{Min/+}$*/Atg16l1[ΔMC]* mice. Cleaved CASP1 level was increased in 11G5-infected $Apc^{Min/+}$*/Atg16l1[ΔMC] vs* 11G5-infected $Apc^{Min/+}$ mice in both colonic mucosa and tumor (Figure 8).

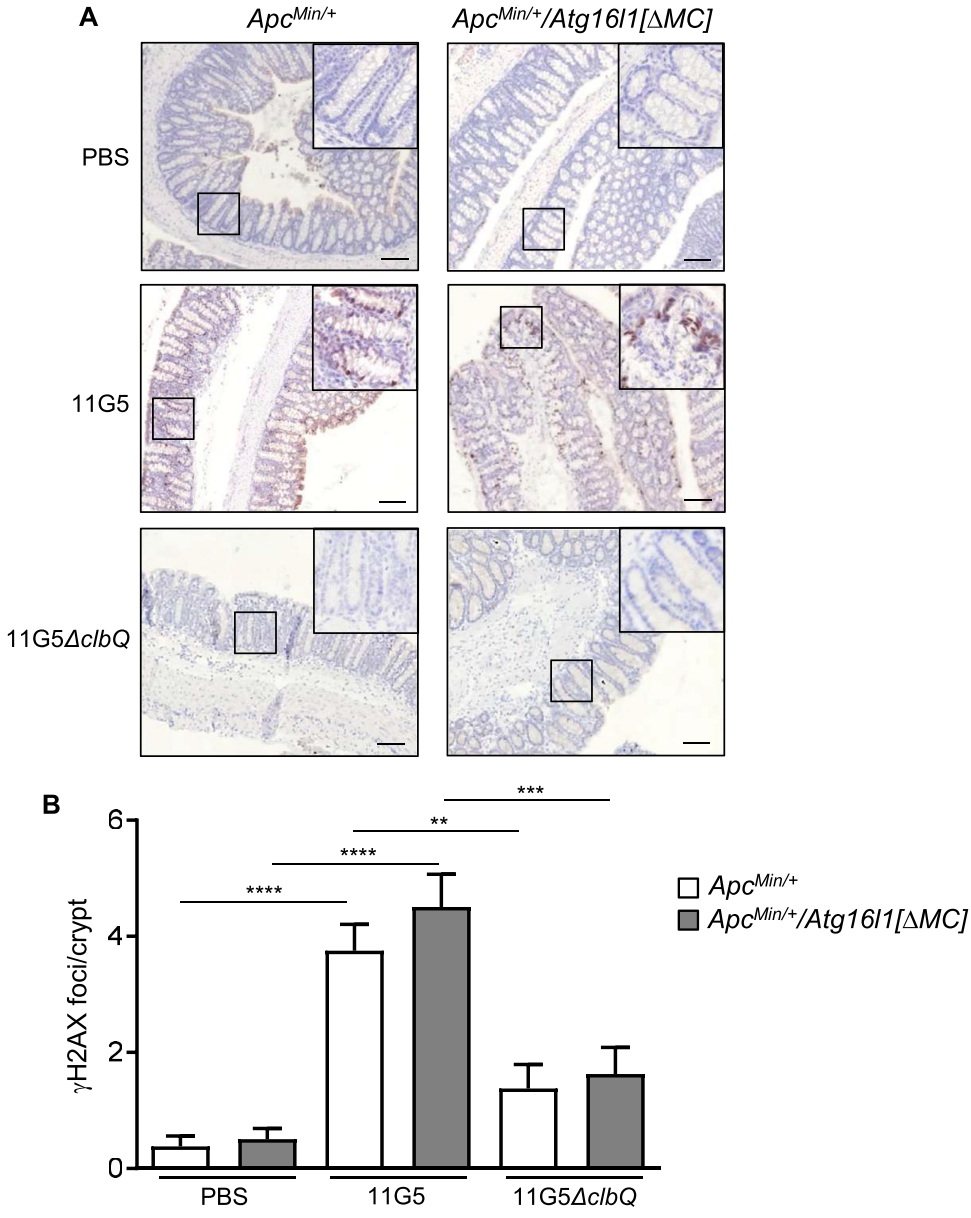

Figure 4. MC-specific *Atg16l1* deficiency did not affect 11G5-induced DNA damage in colonic epithelial cells in $Apc^{Min/+}$ mice. $Apc^{Min/+}$*/Atg16l1[ΔMC]* and $Apc^{Min/+}$ mice were orally administered with PBS or with 10^9 11G5 or 11G5*ΔclbQ* bacteria, and sacrificed at day 65 post-administration. (A) Representative images of immunohistochemical staining for γH2AX in the non-tumoral colonic mucosa. Boxes show magnified fields. Bars: 100 µm. (B) Quantification of γH2AX foci number/crypt determined from 40 crypts/mouse. Values represent means ± SEM. Statistical analysis was performed using one-way Anova test followed by Bonferroni posttest. $^{**}p \leq 0.01$; $^{***}p \leq 0.001$; $^{****}p \leq 0.0001$.

Together, these data, which were in agreement with those obtained with BMDMs, indicated that CoPEC infection induced inflammasome activation dependently of colibactin, leading to increased secreted IL1B level.

MC-specific Atg16l1 deficiency decreased total T cells and cytotoxic CD8$^+$ T cells in the colon of Apc$^{Min/+}$ mice

It was previously reported that the CoPEC 11G5 strain decreases the number of $CD3^+$ total T cells and cytotoxic $CD8^+$ T cells in the colon of $Apc^{Min/+}$ mice in a colibactin-dependent manner [15]. Thus, we analyzed whether MC-specific *Atg16l1* deficiency influenced infiltrating T lymphocyte population, which plays a crucial role in tumorigenesis, by immunofluorescent staining for CD3 or both CD3 and CD8. In agreement with the previous study [15], infection with 11G5, but not 11G5*ΔclbQ*, led to a decrease in the number of $CD3^+$ total T cells and cytotoxic $CD8^+$ $CD3^+$ T cells in both non-tumoral colonic mucosa (Figure 9A, C) and tumors (Figure 9B, D). Under 11G5-infected condition, the numbers of $CD3^+$ total T cells and $CD8^+$ $CD3^+$ T cells were decreased in $Apc^{Min/+}$*/Atg16l1[ΔMC] vs* $Apc^{Min/+}$ mice in both non-tumoral colonic mucosa and tumors. This was not observed under uninfected or 11G5*ΔclbQ*-infected condition (Figure 9). Together, these data showed that MC-specific *Atg16l1* deficiency decreased the numbers of total T cells and cytotoxic $CD8^+$ T cells in the colon of $Apc^{Min/+}$ mice.

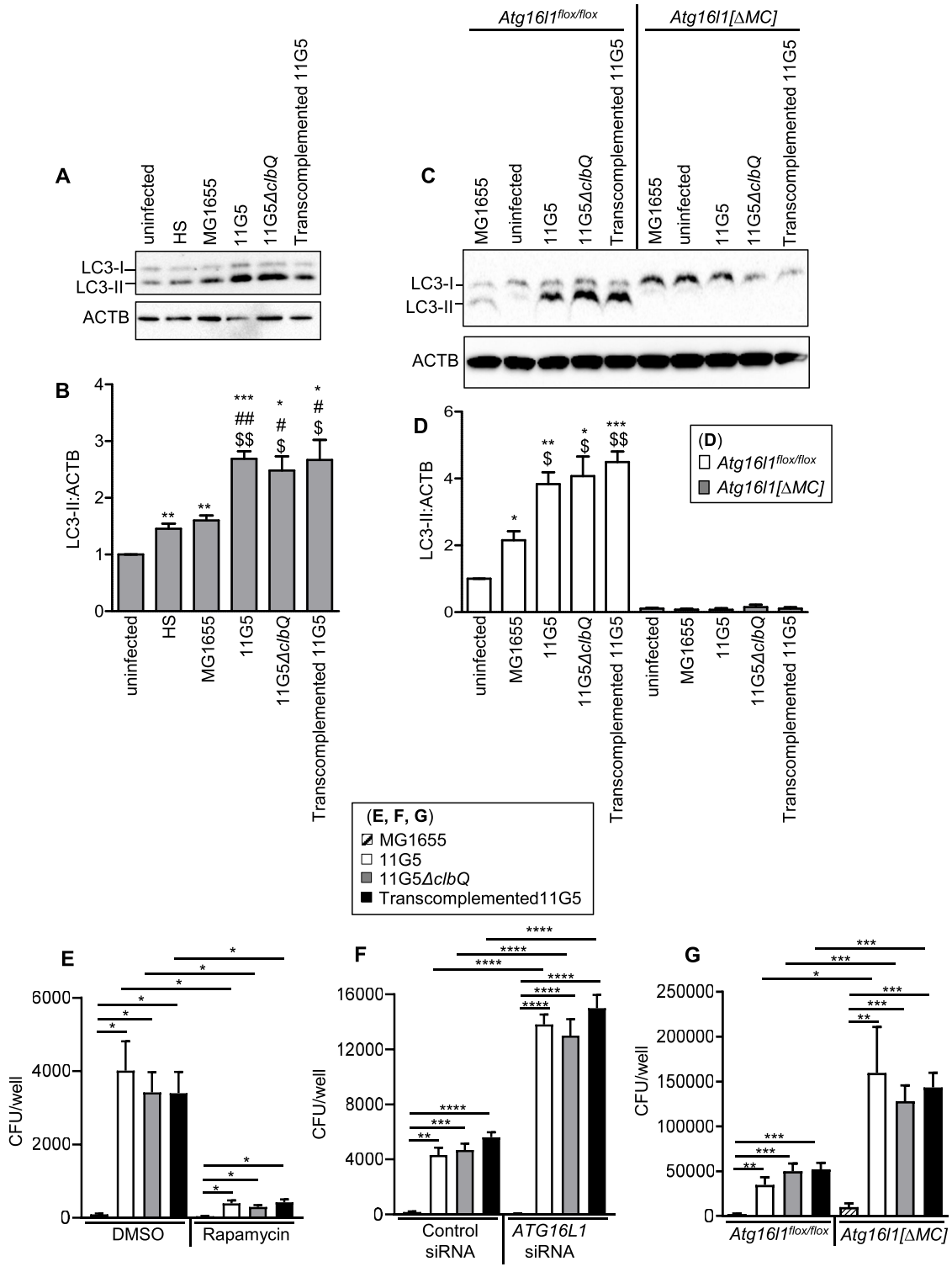

Figure 5. Autophagy was induced in macrophages upon CoPEC infection independently of colibactin, and this was necessary to eliminate intramacrophagic CoPEC bacteria. Human THP-1 macrophages (A, B, E, F) or BMDMs prepared from wild-type (*Atg16l1*$^{flox/flox}$) and *Atg16l1[ΔMC]* mice (C, D, G) were uninfected or infected at a MOI of 100 with one of the following strains: the nonpathogenic commensal *E. coli* strain (MG1655 or HS), the clinical CoPEC 11G5 strain, the isogenic mutant 11G5*ΔclbQ*, the transcomplemented 11G5 strain. After 10 min of centrifugation at 1 000 *g* and a 10 min of incubation at 37°C and 5% CO_2, the infected macrophages were washed three times with PBS and incubated with the culture media containing 100 µg/ml of gentamicin for 40 min, and then changed to culture media containing 50 µg/mL of gentamicin for 8 h. Representative western blot analysis (A, C) and quantification of LC3-II:ACTB/β-actin band intensity from 3 independent blots (B, D). (E) 40 µg/mL rapamycin or vehicle (DMSO) was added together with infection. (F) Cells were transfected with 70 nM of control siRNA or *ATG16L1* siRNA for 2 days before infection. (E-G) to determine the number of intracellular bacteria, the cells were lysed with 1% Triton X-100 in deionized water and plated onto LB agar plates. After 24 h at 37°C, the bacterial CFU were counted. (B, D) ($^{*}p < 0.05$; $^{**}p \leq 0.01$; $^{***}p \leq 0.001$) *vs* uninfected condition; ($^{\#}p < 0.05$; $^{\#\#}p \leq 0.01$) *vs* HS-infected condition; ($^{\$}p < 0.05$; $^{\$\$}p \leq 0.01$) *vs* MG1655-infected condition. (E-G) $^{*}p < 0.05$; $^{**}p \leq 0.01$; $^{***}p \leq 0.001$; $^{****}p \leq 0.0001$. Values represent means ± SEM. Statistical analysis was performed using one-way Anova test followed by Bonferroni posttest.

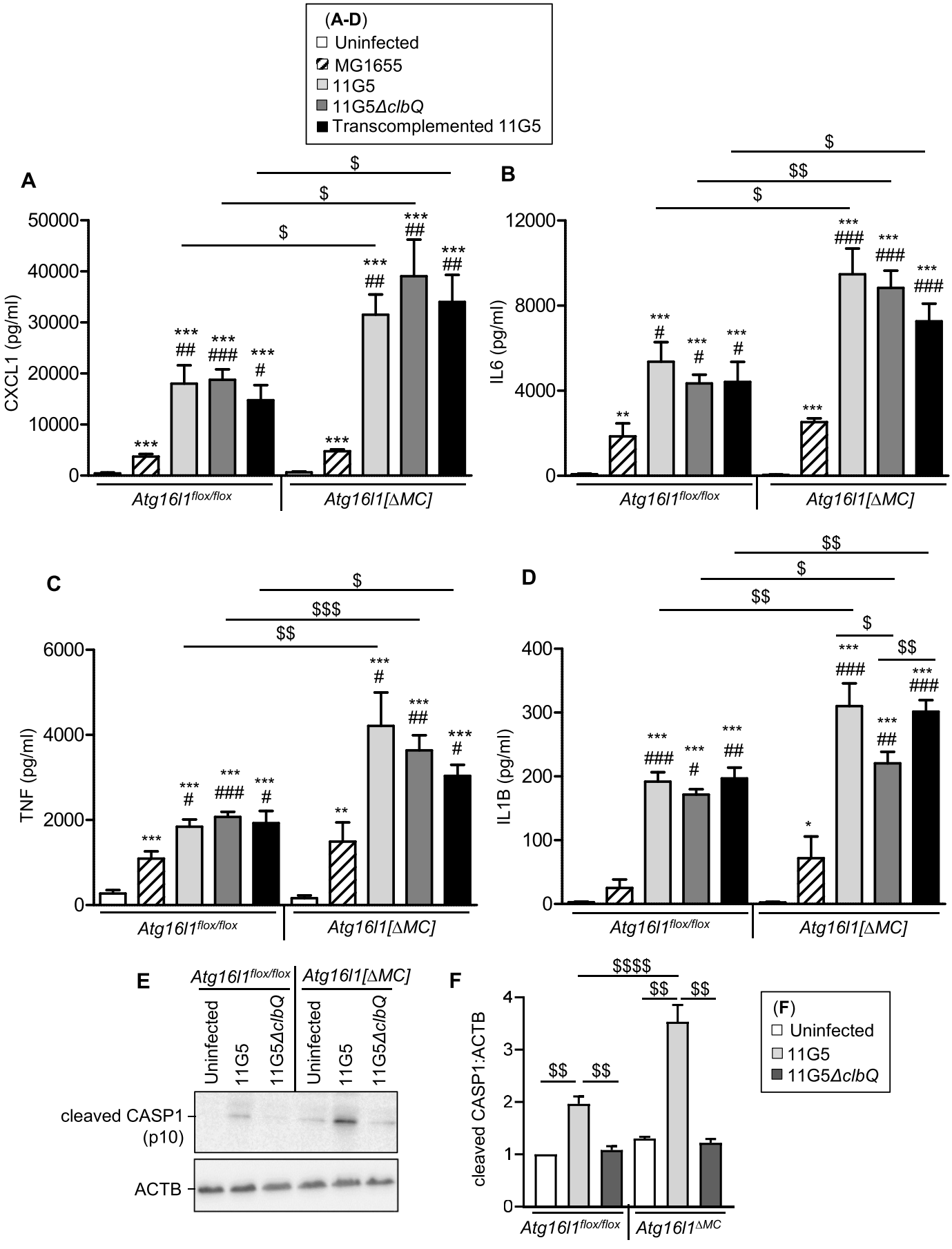

Figure 6. *Atg16l1* deficiency in macrophages led to increases in cleaved CASP1 and secreted IL1B amount upon CoPEC infection dependently of colibactin. BMDMs prepared from wild-type (*Atg16l1*$^{flox/flox}$) and *Atg16l1[ΔMC]* mice were infected with MG1655, 11G5, 11G5*ΔclbQ* or the transcomplemented 11G5 strain at a MOI of

MC-specific Atg16l1 deficiency increased neutrophil infiltration in the colon of Apc$^{Min/+}$ mice

As neutrophils play an important role in CRC development and progression [24], we analyzed whether MC-specific *Atg16l1* deficiency influenced neutrophil infiltration by immunofluorescent staining for the neutrophil-specific surface protein LY6G. As shown in Figure 10, 11G5 infection resulted in an increase in the number of LY6G$^+$ ITGAM$^+$/CD11B$^+$ neutrophils in *Apc$^{Min/+}$* mice compared to uninfected or 11G5*ΔclbQ*-infected condition, in both non-tumoral colonic mucosa (Figure 10A, C) and tumors (Figure 10B, D). Under 11G5-infected condition, the number of LY6G$^+$ ITGAM$^+$ neutrophils infiltrated into the colonic mucosa and tumors were increased in *Apc$^{Min/+}$/Atg16l1[ΔMC] vs Apc$^{Min/+}$* mice (Figure 10). This was not observed under uninfected or 11G5*ΔclbQ*-infected condition (Figure 10). Together, these data showed that MC-specific *Atg16l1* deficiency increased the number of infiltrating neutrophils in the colonic mucosa and tumors of CoPEC-infected *Apc$^{Min/+}$* mice.

Discussion

Autophagy is an important regulator of both innate and adaptive immune responses, and can have a pro- or anti-tumoral context-dependent role in carcinogenesis [25]. We previously showed that *Atg16l1* deficiency in intestinal epithelial cells promotes colorectal carcinogenesis in *Apc$^{Min/+}$* mice under CoPEC-infected condition [9]. As MCs are an important component of the TME, we investigated the role of MC-specific autophagy in colorectal carcinogenesis associated with CoPEC infection. We showed that MC-specific *Atg16l1* deficiency led to an increase in the volume, but not the number, of colonic tumors in *Apc$^{Min/+}$* mice under CoPEC-infected condition. This was accompanied with increased colonic cell proliferation, enhanced inflammasome activation and elevated IL1B secretion, increased infiltrating neutrophil number and decreased total T cell and cytotoxic CD8$^+$ T cell numbers.

In previous studies, we showed that *Atg16l1* deficiency in intestinal epithelial cells enhances the number and volume of colonic tumors in CoPEC-infected *Apc$^{Min/+}$* mice [9] and increases CoPEC-induced formation of invasive carcinomas in a mouse model lacking genetic susceptibility or the use of a carcinogen [13]. Mechanistically, autophagy in intestinal epithelial cells is necessary to inhibit CoPEC-induced DNA damage, which could be implicated in the initiation of tumorigenesis [9, 13]. In this study, we showed that MC-specific *Atg16l1* deficiency did not affect DNA damage in colonic epithelial cells in 11G5-infected *Apc$^{Min/+}$* mice, and this could explain why there was not difference in the tumor number between *Apc$^{Min/+}$/Atg16l1[ΔMC]* and *Apc$^{Min/+}$* mice under 11G5-infected condition. MC-specific *Atg16l1* deficiency increased colonic epithelial cell proliferation in *Apc$^{Min/+}$* mice under 11G5-infected condition. Thus, MC-specific *Atg16l1* deficiency contributes to tumor progression rather than tumor initiation.

In an effort to investigate the mechanism underlying the enhanced tumor volume in 11G5-infected *Apc$^{Min/+}$/Atg16l1 [ΔMC] vs Apc$^{Min/+}$* mice, we isolated BMDMs from *Atg16l1 [ΔMC]* and wild-type *Atg16l1$^{flox/flox}$* mice as macrophages are one of the predominant tumor-infiltrating myeloid cells supporting key processes in tumor progression [16]. We found that CoPEC infection induced autophagy activation in macrophages independently of colibactin. Although *Atg16l1* deficiency led to increased 11G5 number in BMDMs, this was also observed for the mutant 11G5*ΔclbQ*. In particular, the intracellular numbers of 11G5 and 11G5*ΔclbQ* were not significantly different either in BMDMs from *Atg16l1[ΔMC]* mice or BMDMs from wild-type mice. *In vivo*, the colonization of mouse colon by 11G5 or 11G5Δ*clbQ* was also similar in both *Apc$^{Min/+}$* and *Apc$^{Min/+}$/Atg16l1[ΔMC]* mice. This suggested that the increase in tumor size in 11G5-infected *Apc$^{Min/+}$/Atg16l1[ΔMC] vs* 11G5*ΔclbQ*-infected *Apc$^{Min/+}$/Atg16l1[ΔMC]* mice was not due to increased bacterial colonization in the colon.

As inflammation has been associated with enhanced tumorigenesis [26], we analyzed the impact of MC-specific *Atg16l1* deficiency on the amounts of secreted pro-inflammatory cytokines and chemokine. In BMDMs, we showed that 11G5 infection increased the amounts of secreted IL1B, IL6, TNF and CXCL1, and this was further enhanced by *Atg16l1* deficiency. Interestingly, among them, only the secreted IL1B amount was increased in 11G5-infected *vs* 11G5*ΔclbQ*-infected condition in BMDMs from *Atg16l1[ΔMC]* mice. *In vivo* data agreed with the *in vitro* data, showing increased secreted IL1B amount in the colonic mucosa from 11G5-infected *Apc$^{Min/+}$/Atg16l1[ΔMC]* mice compared to 11G5*ΔclbQ*-infected *Apc$^{Min/+}$/Atg16l1[ΔMC]* mice or 11G5-infected *Apc$^{Min/+}$* mice. These indicated that CoPEC-induced IL1B secretion was partly dependent on colibactin in MCs with *Atg16l1* deficiency, and this could be one of the mechanisms underlying the enhanced cellular proliferation and increased tumor volume in 11G5-infected *vs* 11G5*ΔclbQ*-infected *Apc$^{Min/+}$/Atg16l1[ΔMC]* mice. Pharmaceutical or genetic approaches targeting IL1 receptor signaling pathway would be of interest to validate the involvement of IL1B in the pro-tumoral effect of colibactin.

Indeed, a role for IL1B in cancer has been shown [27]. IL1B, once secreted, can target several cell types by binding to IL1 receptor, leading to activation of the downstream signaling pathways. Among them, activation of MAPK/p38 and

100. After 10 min of centrifugation at 1 000 *g* and a 10 min of incubation at 37°C and 5% CO_2, the infected macrophages were washed three times with PBS and incubated with the culture media containing 100 µg/mL of gentamicin for 40 min, and then changed to culture media containing 50 µg/mL of gentamicin for 8 h. (A-D) Secreted IL6, IL1B, TNF and CXCL1 levels in cell culture supernatant were quantified by ELISA. Representative western blot analysis (E) and quantification of cleaved CASP1 (p10 subunit):ACTB/β-actin band intensity from 3 independent blots (F). (A-D) (*$p < 0.05$; **$p \leq 0.01$; ***$p \leq 0.001$) *vs* uninfected condition; ($^{\#}p < 0.05$; $^{\#\#}p \leq 0.01$: $^{\#\#\#}p \leq 0.001$) *vs* MG1655-infected condition; $^{\$}p < 0.05$; $^{\$\$}p \leq 0.01$; $^{\$\$\$}p \leq 0.001$; $p \leq 0.0001$. (F) $^{\$\$}p \leq 0.01$; $^{\$\$\$\$}p \leq 0.0001$. Values represent means ± SEM. Statistical analysis was performed using one-way Anova test followed by Bonferroni posttest.

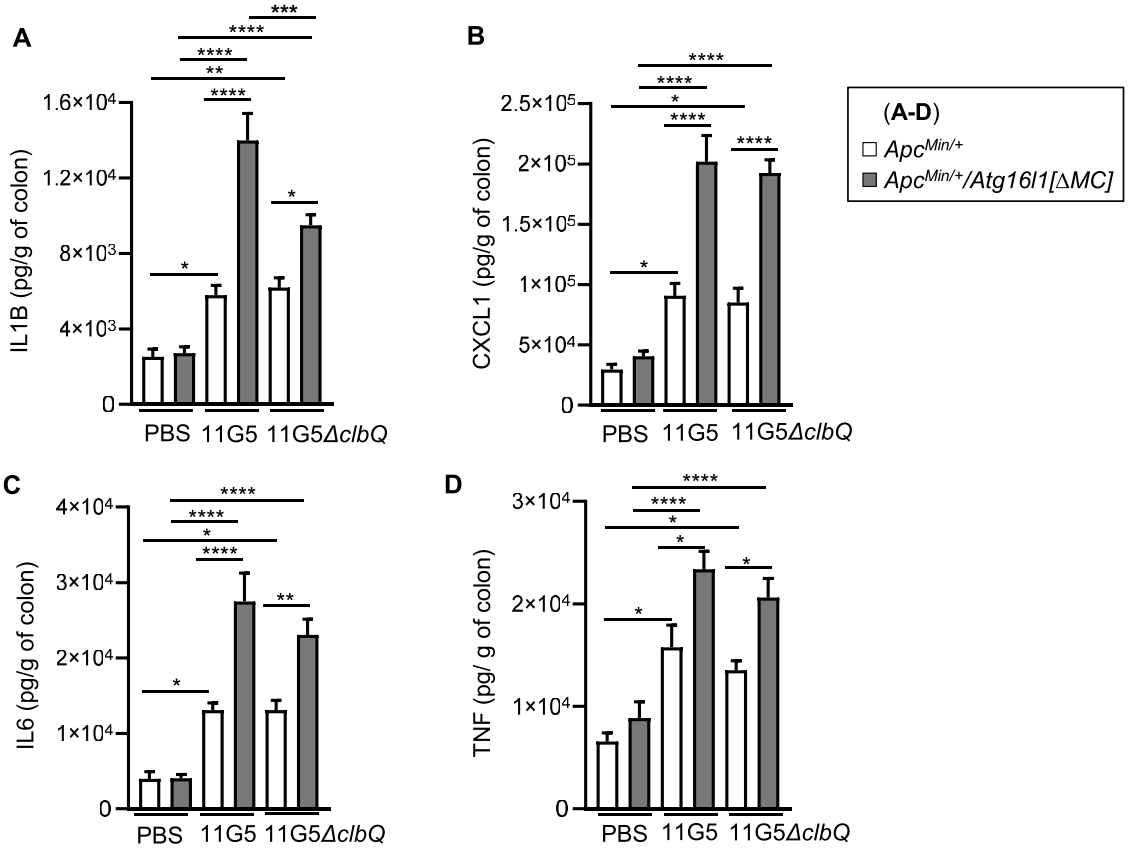

Figure 7. MC-specific *Atg16l1* deficiency increased secreted IL1B amount in the colon of $Apc^{Min/+}$ mice upon CoPEC infection dependently of colibactin. $Apc^{Min/+}$*/Atg16l1[ΔMC]* and $Apc^{Min/+}$ mice were orally administered with PBS or with 10^9 11G5 or 11G5*ΔclbQ* bacteria, and sacrificed at day 65 post-administration. Secreted IL1B, IL6, TNF and CXCL1 amounts in the colonic culture supernatant were quantified by ELISA. Values represent means ± SEM. Statistical analysis was performed using one-way Anova test followed by Bonferroni posttest. *$p < 0.05$; **$p \leq 0.01$; ***$p \leq 0.001$; ****$p \leq 0.0001$.

NFKB/NF-κB pathways leads to the transcription of target genes involved in several biological processes [27]. Thus, IL1B has been implicated in angiogenesis, cancer cell proliferation, migration, and metastasis. Concerning CRC, it has been shown that in human colon cancer cells, IL1B upregulates *MIR181A* level, which is responsible for PTEN (phosphatase and tensin homolog) repression and cell proliferation induction [28]. Macrophage-derived IL1B has been shown to stimulate WNT signaling and the growth of colon cancer cells *via* the inactivation of GSK3B (glycogen synthase kinase 3 beta) [29].

The activation of inflammasomes, specifically the most fully characterized NLRP3 (NLR family, pyrin domain containing 3) inflammasome, is required for the activation of CASP1 responsible to cleave pro-IL1B into mature IL1B [30] Previous studies showed that dysfunctional autophagy leads to abnormal inflammasome activation, which is associated with increased CASP1 activity, elevated IL1B production and higher susceptibility to experimental intestinal inflammation in mice [10]. In line with this, we showed that CoPEC infection induced inflammasome activation dependently of colibactin, and this could be the mechanism underlying the colibactin-induced IL1B secretion. Indeed, inflammasomes can be activated by a variety of infectious stimuli, including microbes-derived signals, such as bacterial-derived toxins, and host-derived signals (*e.g.*, ion flux, mitochondrial dysfunction, reactive oxygen species, or metabolic factors) [31]. The exact mechanism by which colibactin mediates inflammasome activation requires further study. Nonetheless, our data suggested that ATG16L1 in myeloid cells is necessary to inhibit colibactin-mediated inflammasome activation and subsequently IL1B secretion, and this might contribute to the tumor suppressor role of autophagy under CoPEC-infection condition.

Furthermore, we showed that MC-specific *Atg16l1* deficiency resulted in an increase in the numbers of infiltrating neutrophil in the colonic mucosa and tumors upon CoPEC infection in a colibactin-dependent manner. Tumor-associated neutrophils are an important component of the tumor immune microenvironment, as they have key regulatory role in the carcinogenesis, proliferation and metastasis of CRC [24]. A significant cytokine secreted by neutrophils is IL1B [32]. IL1B has been shown to play a role in the regulation of neutrophil recruitment through the induction of chemokine production (including IL8) *via* the NFKB pathway [33]. Thus, it is reasonable to hypothesize that the colibactin-induced IL1B secretion by neutrophils may have a feedback regulation role in neutrophil recruitment into the colonic tumors.

Furthermore, we showed that MC-specific *Atg16l1* deficiency led to a decrease in the numbers of total T cells and

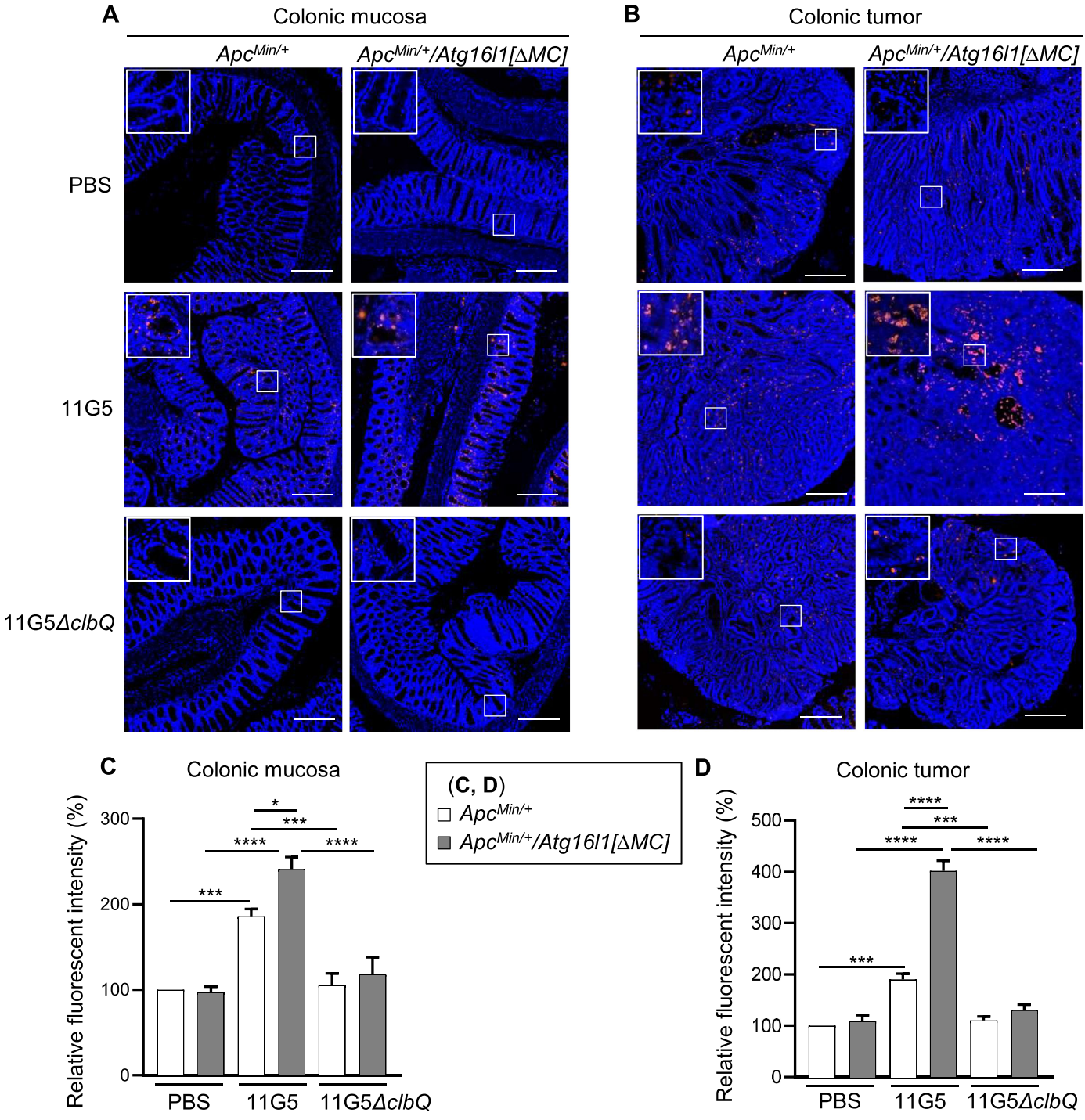

Figure 8. MC-specific *Atg16l1* deficiency increased cleaved CASP1 levels in the colon of $Apc^{Min/+}$ mice upon CoPEC infection dependently of colibactin. $Apc^{Min/+}$*/Atg16l1[ΔMC]* and $Apc^{Min/+}$ mice were orally administered with PBS or with 10^9 11G5 or 11G5*ΔclbQ* bacteria, and sacrificed at day 65 post-administration. Representative images of immunofluorescent staining for cleaved CASP1 (red) in the non-tumoral colonic mucosa (A) and tumors (B). Nuclei were stained with Hoechst (blue). Boxes show magnified fields. Bars: 200 µm. Quantification of cleaved CASP1 fluorescence intensity, normalized to Hoechst intensity, in the colonic mucosa (C) and tumor (D), was presented as a percentage of the value defined for the $Apc^{Min/+}$ + PBS group (100%). Values represent means ± SEM. Statistical analysis was performed using one-way Anova test followed by Bonferroni posttest. *$p < 0.05$; ***$p \leq 0.001$; ****$p \leq 0.0001$.

cytotoxic $CD8^+$ T cells in $Apc^{Min/+}$ mice upon CoPEC infection in a colibactin-dependent manner. Given the well described cytotoxic anti-tumoral function of $CD8^+$ T cells [16], our results suggested that ATG16L1 in MCs was necessary for anti-tumor T cell response in colorectal carcinogenesis associated with CoPEC infection. Our findings are supported by other studies showing that several bacteria potentially modulate T cell response, thereby controlling CRC progression. For example, it was shown that the human colonic commensal bacteria enterotoxigenic *Bacteroides fragilis* promote colon tumorigenesis in $Apc^{Min/+}$ mice *via* activation of T helper 17 cell responses [34]. A

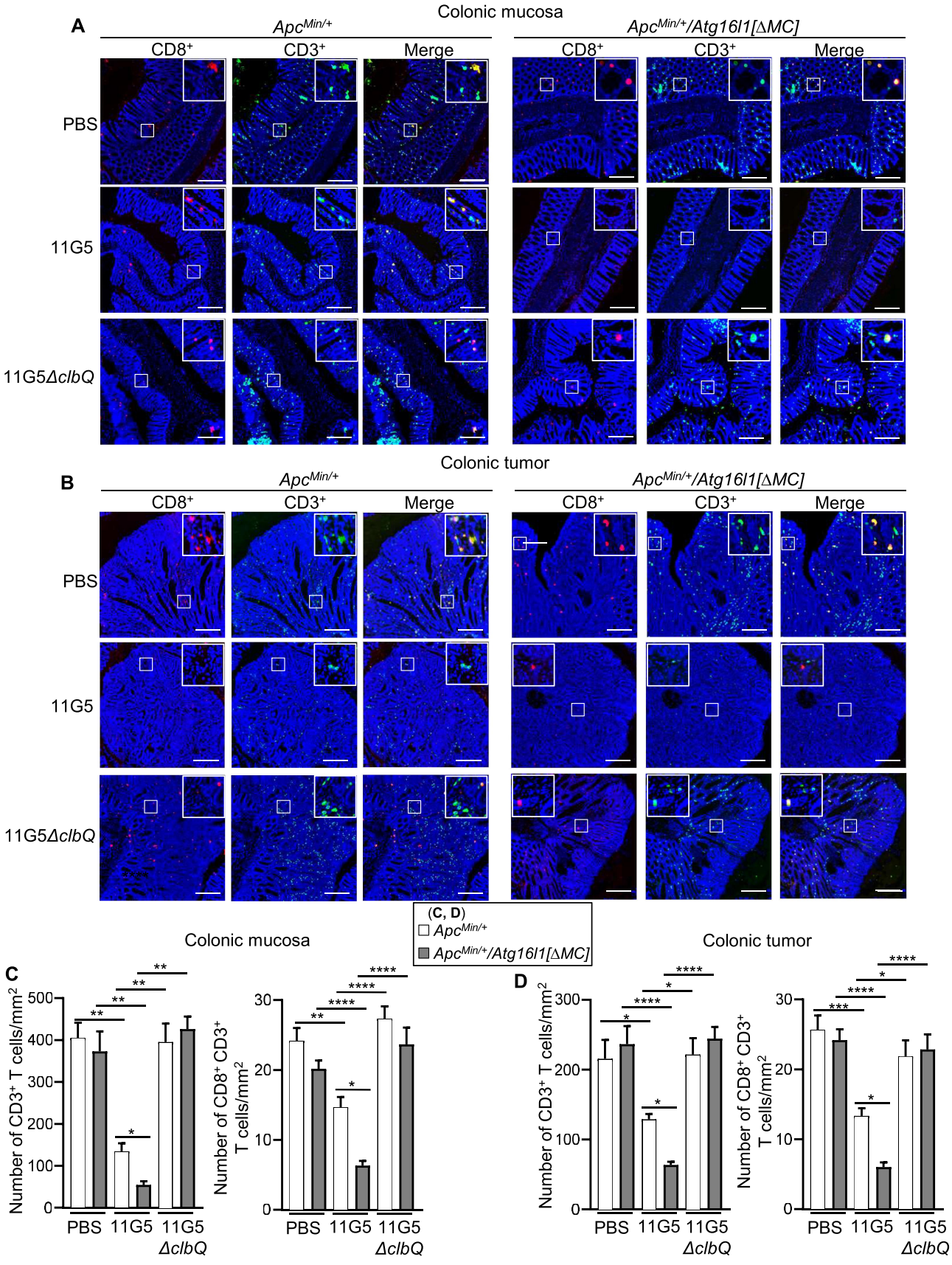

Figure 9. MC-specific *Atg16l1* deficiency decreased $CD3^+$ total T cell and cytotoxic $CD8^+$ T cell numbers in the colon of $Apc^{Min/+}$ mice upon CoPEC infection dependently of colibactin. $Apc^{Min/+}$/*Atg16l1[ΔMC]* and $Apc^{Min/+}$ mice were orally administered with PBS or with 10^9 11G5 or 11G5*ΔclbQ* bacteria, and sacrificed at day 65 post-administration. Representative images of CD8 (red) and CD3 (green) immunofluorescent double staining in the colonic mucosa (A) and tumors (B). Nuclei were stained with Hoechst (blue). Bars: 200 µm. Boxes show magnified fields. Quantification of $CD3^+$ total T cell and $CD8^+$ $CD3^+$ T cell number/mm^2 of colonic mucosa (C) or tumor (D). Values represent means ± SEM. Statistical analysis was performed using one-way Anova test followed by Bonferroni posttest. *$p < 0.05$; **$p \leq 0.01$; ***$p \leq 0.001$; ****$p \leq 0.0001$.

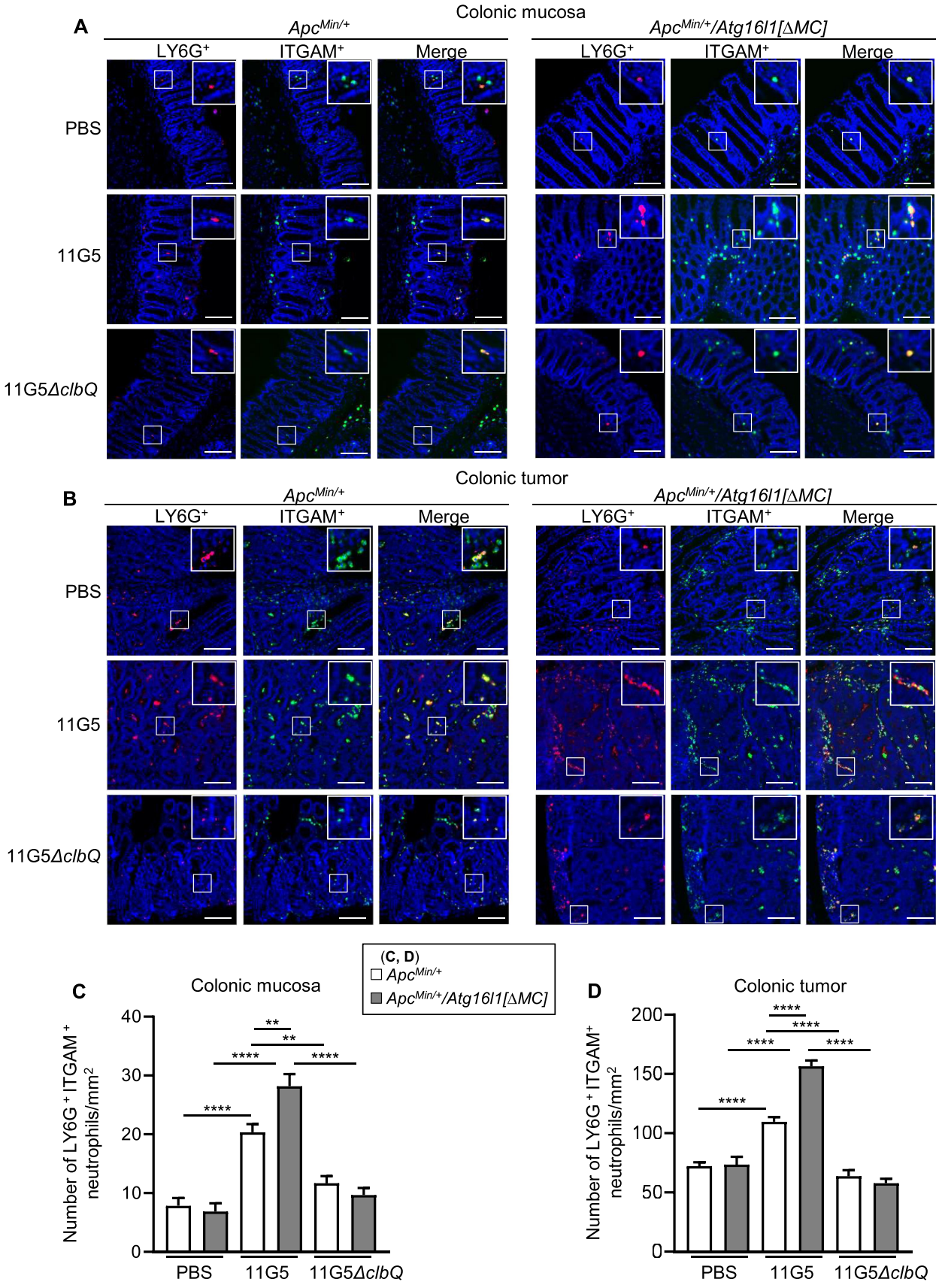

Figure 10. MC-specific *Atg16l1* deficiency increased neutrophil infiltration in the colonic mucosa and tumor of $Apc^{Min/+}$ mice upon CoPEC infection dependently of colibactin. $Apc^{Min/+}$*/Atg16l1[ΔMC]* and $Apc^{Min/+}$ mice were orally administered with PBS or with 10^9 11G5 or 11G5*ΔclbQ* bacteria, and sacrificed at day 65 post-administration. Representative images of LY6G (red) and ITGAM (green) immunofluorescent double staining in the colonic mucosa (A) and tumors (B). Nuclei were stained with Hoechst (blue). Bars: 100 µm. Boxes show magnified fields. Quantification of $LY6G^+$ $ITGAM^+$ neutrophil number/mm^2 of colonic mucosa (C) or tumor (D). Statistical analysis was performed using one-way Anova test followed by Bonferroni posttest. $^{**}p \leq 0.01$; $^{***}p \leq 0.001$; $^{****}p \leq 0.0001$.

susceptible mouse model of colorectal tumorigenesis colonized with enterotoxigenic *Bacteroides fragilis* exhibits a distinct immune TME with tumors infiltrated by $CD8^+$ T cells [35]. It was recently shown that tissue-resident commensal bacteria *Ruminococcus gnavus* and *Blautia producta*, which belong to the *Lachnospiraceae* family, promote the activation of $CD8^+$ T cells and reduce colon tumor growth in immunocompetent mice [36].

It leaves to investigate if the increased inflammasome activation and impaired anti-tumor T cell response given by *Atg16l1* deficiency in MCs is interconnected or independent. Blocking the IL1 receptor signaling pathway, by pharmaceutical or genetic approaches, and examining whether anti-tumor T cell response is impaired upon *Atg16l1* deficiency in MCs could be considered to answer this important point.

It is worthy to note that several autophagy-independent functions of ATG16L1, defined as those that do not involve LC3/GABARAP lipidation, have been reported [37]. Thus, we cannot exclude the possibility that *Atg16l1* deficiency in MCs might have an impact on another autophagy-independent process, and this could subsequently contribute to tumorigenesis. In addition, the difference in the tumorigenesis between $Apc^{Min/+}$/*Atg16l1[ΔMC]* and $Apc^{Min/+}$ mice was observed in $Apc^{Min/+}$ mouse model, and an additional model, such as a syngeneic model of CRC, could be interesting to evaluate whether the conclusion is dependent on the *Apc* mutation or not. Nonetheless, it is worthy to note that the *in vitro* experiments, which showed the role of ATG16L1 in limiting colibactin-induced inflammasome activation and IL1B secretion, were performed using the BMDMs from *Atg16l1[ΔMC]* and WT mice (without *Apc* mutation).

Altogether, our results indicated that *Atg16l1* deficiency in MCs led to increased tumor volume in $Apc^{Min/+}$ mice under 11G5-infected condition, and this was associated with increased inflammasome activation and enhanced IL1B secretion, increased neutrophil infiltration as well as impaired anti-tumor T cell response and increased colonic epithelial cell proliferation (Figure 11). These data suggested that autophagy in MCs was necessary to inhibit colonic tumor growth under CoPEC colonization condition.

Materials and methods

Bacterial strains

The commensal *E. coli* strains MG1655 or HS, the clinical 11G5 strain, the isogenic mutant 11G5*ΔclbQ* (depleted for the *clbQ* gene in the *pks* island and unable to produce colibactin) and the transcomplemented strain 11G5*ΔclbQ*+*clbQ* [9] were used. Bacteria were grown at 37°C in Luria-Bertani (LB; Condalab, 1551.00) medium overnight.

Animal model and infection

Mice with MC-specific *Atg16l1* deficiency (*Atg16l1[ΔMC]*) were generated by crossing mice bearing a *loxP* site flanked exon 1 of the *Atg16l1* gene ($Atg16l1^{flox/flox}$ mice [38]) with mice expressing the Cre recombinase gene under the control of the *Lyz2/LysM* (lysozyme 2) promoter (*Lyz2-Cre* mice) [39] (The Jackson Laboratory, 004781). *Atg16l1[ΔMC]* mice and their control littermates $Atg16l1^{flox/flox}$ were crossed with $Apc^{Min/+}$ mice (C57BL/6J; The Jackson Laboratory) to generate $Apc^{Min/+}$/$Atg16l1^{flox/flox}$ and $Apc^{Min/+}$/*Atg16l1[ΔMC]* mice. Mice were infected with 11G5 or 11G5*ΔclbQ* as previously described [9]. Briefly, mice were given 2.5 g/l streptomycin (Euromedex, 1121) in drinking water during 3 days, and then received regular water for 1 day. Each mouse was orally administrated by gavage with 10^9 bacteria in 200 µl PBS (Gibco, 14190–094) or with PBS alone (uninfected condition). Body weight was determined at different days post-infection. Feces harvested at different days post-infection were weighed, crushed in 500 µl of PBS and spread on LB agar (Condalab, 1800.00) supplemented with 50 µg/ml ampicillin (Euromedex, EU0400) and 50 µg/ml kanamycin (Euromedex, UK0015) to select 11G5, or with 50 µg/ml ampicillin, 50 µg/ml kanamycin and 100 µg/ml spectinomycin (Sigma-Aldrich, S4014) to select 11G5*ΔclbQ*. After 24 h at 37°C, the colony-forming units (CFU) of bacteria were counted and normalized to gram of feces.

Mice were sacrificed at day 65 post-infection. Colonic tumor number and volume ([width^2 × length]/2) were determined using a dissecting microscope. One part of the colon was swiss-rolled and fixed in buffered 10% formalin (Sigma-Aldrich, HT501128) and embedded in paraffin, and the other part was frozen at −80°C for RNA and protein extraction.

Cell culture

The human monocyte cell line THP-1 (ATCC, TIB-202) was maintained in an atmosphere containing 5% CO_2 at 37°C in RPMI medium 1640 (Gibco, 31870–025) containing 10% fetal bovine serum (Dominique Dutscher, S1900) and 1% glutamine (Gibco, 25030–024). THP-1 monocytes were differentiated into macrophages by an 18 h treatment with 20 ng/ml phorbol mysristate acetate (Sigma-Aldrich, P8139). Primary BMDMs were extracted from tibia and femur of $Atg16l1^{flox/flox}$ and *Atg16l1[ΔMC]* mice. Cells were grown in RPMI medium supplemented with 10% fetal bovine serum, 1% glutamine, 1% HEPES, pH 7.2–7.4 (Dominique Dutscher, L0180), 0.1% β-mercaptoethanol (Gibco, 31350–010), 1 mM sodium pyruvate (PAA laboratories, SH30239.01), 1% penicillin-streptomycin (Hyclone, SV30079.01) and 20% of L929 cell-conditioned medium (ATCC, CCL-1). After 3 days of culture, fresh medium was added. On day 7, cells were washed and seeded in complete medium without antibiotics and incubated for 24 h before bacterial infection.

Infection and survival assay

The ability of bacteria to survive and replicate within the macrophages was determined by the gentamycin protection assay. THP-1 macrophages and BMDMs were infected with bacteria at a multiplicity of infection (MOI) of 100 in the culture medium without antibiotics. After 10 min of centrifugation at 1 000 *g* and a 10 min of incubation at 37°C and 5%

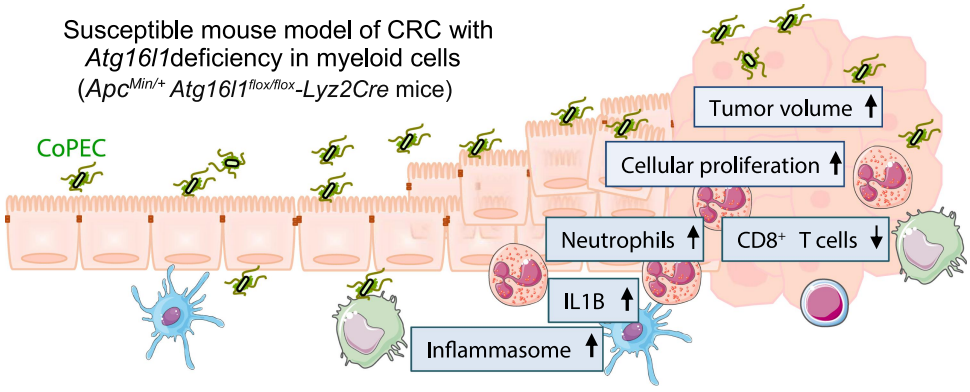

Figure 11. Proposed model for the role of ATG16L1 in MCs in colorectal carcinogenesis associated with CoPEC colonization. ATG16L1 in MCs is necessary to inhibit the colonic tumor growth in a mouse model of CRC infected with CoPEC. Mechanistically, ATG16L1 dysfunction in MCs leads to increased colorectal tumor volume, which is accompanied with increased colibactin-induced inflammasome activation and IL1B secretion, increased neutrophil infiltration and decreased anti-tumor $CD8^+$ T cells in the colonic mucosa and tumors, and increased colonic epithelial cell and cancer cell proliferation.

CO_2, the infected macrophages were washed three times with PBS and incubated with the culture media containing 100 µg/ml of gentamicin for 40 min. After three washes, fresh culture medium containing 50 µg/ml of gentamicin was added for the indicated time. To determine the number of intracellular bacteria, the cells were washed three times with PBS, lysed with 1% Triton X-100 (Sigma-Aldrich, G-1264) in deionized water, diluted and plated on LB agar plates. After one night at 37°C, the CFU were counted. Whenever indicated, THP-1 macrophages were treated with 40 µg/ml of rapamycin together with infection, and rapamycin was kept together with the cells until lysis. For experiments with bafilomycin A1 treatment, cells were treated with bafilomycin A1 (Sigma-Aldrich, 19–148) 30 min prior infection at 100 nM.

Transfection of siRNA

Scramble siRNA (Ambion, AM4611) and *ATG16L1* siRNA (Dharmacon, L-021033-01) were used. THP-1 cells were transfected with vehicle or 70 nM of specific siRNA using Lipofectamine 2000 (Invitrogen, 11668027) and Opti-MEM I reduced serum (Invitrogen 319,885,062). After 6 h, the cells were washed and incubated with the culture medium for 48 h.

Western blot analysis

Extraction of protein from cells in culture or tissue samples and western blot analysis were performed as previously described[9]. The relevant primary antibodies used were: anti-LC3 (Sigma-Aldrich, L8918), anti-cleaved CASP1 (Invitrogen, PA5–105049), anti-SQSTM1/p62 (Santa Cruz Biotechnology, sc-28,359), anti-PCNA (Cell Signaling Technology, 13110) and anti-ACTB/β-actin (Cell Signaling Technology, 4970). The HRP-conjugated secondary antibodies anti-rabbit IgG (Cell Signaling Technology, 7074) and anti-mouse IgG (Cell Signaling Technology, 7076) were used. Blots were detected using the Clarity Western ECL Substrate (Bio-Rad, 170–5060) and revealed using the ChemiDocTM XRS System (Bio-Rad).

Total RNA extraction, cDNA synthesis and qRT-PCR

Total RNAs were extracted from the mouse colonic mucosa samples using RNeasy kit (Qiagen, 74104), and were reversely transcribed using the SensiFast™ cDNA Synthesis Kit (Bioline, BIO-65054) according to the manufacturer's instruction. qRT-PCR was performed using 4 µl of cDNA, SsoAdvanced Universal SYBR Green Supermix (Bio-Rad, 1725274) and 200 nM of specific primers (Table S1) using a thermocycler (Bio-Rad) according to the following program: 95°C-30 s followed by 40 cycles of (90°C-5 s and 60°C-30 s). *Rplp0/36b4* was used as internal control. Fold-induction was calculated using the *Ct* method as follow: $\Delta\Delta Ct = (Ct_{\text{target gene}} - Ct_{\text{housekeeping gene}})_{\text{test condition}} - (Ct_{\text{target gene}} - Ct_{\text{housekeeping gene}})_{\text{normalized condition}}$, and the final data were derived from $2^{-\Delta\Delta Ct}$.

Enzyme-linked Immunosorbent Assays (ELISA)

The amount of CXCL1, TNF, IL1B or IL6 secreted into the supernatants from cells in culture and colonic tissues cultured for 24 h in RPMI medium containing 1% penicillin-streptomycin and 100 µg/ml gentamicin in an atmosphere containing 5% CO_2 at 37°C was determined by ELISA (R&D systems, mouse CXCL1/KC DuoSet ELISA, DY453; mouse IL6 DuoSet ELISA, DY406; mouse IL1B DuoSet ELISA, DY401; mouse TNF-alpha DuoSet ELISA, DY410) according to the manufacturer's instructions.

Hematoxylin and eosin staining and histological examination

Mouse colons were embedded in paraffin and cut into 5-µm sections with a microtome, and colonic sections were H&E-stained. The histological evaluation of the colonic sections was performed under blinded conditions by an expert anatomo pathologist according to the criteria in Table S2.

Immunohistochemical staining

The colonic sections were deparaffined in HISTO-CLEAR (Electron Microscopy Sciences, 64110–04) for 15 min (2 times), rehydrated in ethanol diminishing gradient (100%, 96%, 75% and water: 1 min each) and unmasked in Tris-EDTA buffer (10 mM Tris-Base, 1 mM EDTA, pH 9) during 20 min at 95°C. The sections were incubated with blocking buffer (1% bovine serum albumin [Euromedex, 04–100812-E] in PBS) for 1 h at room temperature and then with anti-phopho-H2AX (dilution 1:500; Cell Signaling Technology, 9718), or anti-MKI67/Ki67 (dilution 1:500; Cell Signaling Technology, 12202S) overnight at 4°C. After several washes with PBS, the sections were incubated with the corresponding secondary antibody coupled with peroxydase (dilution 1:500; Jackson Immunoresearch, 111-065-003) for 2 h at room temperature. Revelation was performed using 3,3'-diaminobenzidine (NovaRED; Vector Laboratories, SK-4800). The sections were counterstained with Mayer's hematoxylin solution (Sigma-Aldrich, MHS32) for 10 sec, rinsed under running water, dehydrated and mounted using a 50:50 PBS-glycerol solution. The microscopic images were acquired using the Scanner Zeiss Axioscan Z1 (Zeiss) and analyzed using ZEN 2 software.

Immunofluorescent staining

The colonic sections were deparaffined in Histoclear for 15 min (2 times), rehydrated in ethanol diminishing gradient (100%, 96%, 75% and water: 1 min each) and unmasked in Tris-EDTA buffer (10 mM Tris-Base, 1 mM EDTA, pH 9) during 20 min at 95°C for CD3, CD8 LY6G, ITGAM/CD11B and LC3 staining, or in citrate buffer (10 mM citrate, pH 6) during 30 min at 95°C for cleaved CASP1 staining.

The sections were then incubated with the blocking buffer (1X PBS containing 2.5% horse serum (Vector Laboratories, 30022) for cleaved CASP1 staining, 5% fetal bovine serum for CD8 staining, 5% normal goat serum (Vector Laboratories, 30023) for LY6G staining, or 5% horse serum (Vector Laboratories, 30022) and 0.3% Triton X-100 (Sigma-Aldrich, G-1264) for LC3 staining) for 2 h (cleaved CASP1 or CD8 staining) or 1 h (LY6G or LC3 staining) at room temperature. The sections were then incubated with anti-cleaved CASP1 (dilution 1:400; Invitrogen, PA5–105049), anti-CD8 (dilution 1:50; Invitrogen, MA1–145), anti-LY6G (dilution 1:100; Biolegend, 127602) or anti-LC3 (dilution 1:400, Cell Signaling Technology, 4108S) antibody overnight at 4°C. After several washes with PBS, the sections were incubated with the corresponding HRP-conjugated secondary antibodies, then the signal was amplified using the Immpress HRP-conjugated anti-rabbit IgG (Vector Laboratories, MP-7401-15) or the Immpress HRP-conjugated anti-rat IgG (Vector Laboratories, MP-7444-15) and the TSA (Tyramide Signal Amplification) revelation kit (Alexa Fluor 555; Invitrogen, B40955).

A second staining was then performed for the sections that were stained with CD8 or LY6G (to generate CD8 CD3 or LY6G ITGAM double staining). The sections were incubated for 20 min with 0.02 N HCl to block peroxidases. They were then placed in a blocking buffer (1X PBS containing 3% bovine serum albumin and 0.025% Triton-100X for CD3 staining, or 5% horse serum and 0.3% Triton-100X for ITGAM staining) for 2 h (CD3 staining) or 1 h (ITGAM staining) at room temperature. They were then incubated overnight at 4°C with the anti-CD3E/CD3ε (dilution 1:300; Cell Signaling Technology, 99940T) or anti-ITGAM (dilution 1:100; Cell Signaling Technology, 17800S). As described previously, the sections were incubated with the corresponding HRP-conjugated secondary antibodies, then amplified using the Immpress anti-rabbit polymer HRP (Vector Laboratories, MP-7401-15) and the TSA revelation kit (Alexa Fluor 647; Invitrogen, B40958). Finally, slides were mounted using a 50:50 PBS-glycerol solution. The microscopic images were acquired using the Scanner Zeiss Axioscan Z1 (Zeiss) and analyzed using ZEN 2 software.

Ethics statement

Animal protocols were conducted in accordance with the recommendations of the Guide for the Care and Use of Laboratory Animals of the University of Clermont Auvergne and were approved by the French Ministry of Higher Education and Research (APAFIS #11254).

Statistical analysis

Results are presented as mean ± standard error of the mean (SEM). Statistical analyses were performed using the ANOVA test followed by a posttest Bonferroni correction (Kruskal-Wallis if not parametric) with GraphPad Prism 9. A p value less than 0.05 was considered statistically significant.

Acknowledgements

We would like to thank Professor Philip Rosenstiel (Institute of Clinical Molecular Biology, Christian-Albrechts-University and University Hospital Schleswig-Holstein, Kiel, Germany) for kindly providing the *Atg16l1*$^{flox/flox}$ mice. We thank the platforms CLIC (Clermont Imagerie Confocale, iGReD, Université Clermont Auvergne) for assistance with confocal microscopy and CICS (Centre Imagerie Cellulaire Santé, Université Clermont Auvergne) for assistance with tissue preparation. We also thank Groupe Cancer Clermont Auvergne. We thank Christelle Soubeyrand-Damon (Anipath histology platform, iGReD, Université Clermont Auvergne) for her help with immunohistochemical and immunofluorescent staining. We thank Dr. Elisabeth Billard (M2iSH, Université Clermont Auvergne) for her valuable advices, and several members of M2iSH, U1071 Inserm unit (Cécily Lucas, Anaïs Larabi, Alexandra Rezard, Sandra Lebeau and Hanh Hoang) for their help with *in vivo* experiments.

Disclosure statement

No potential conflict of interest was reported by the author(s).

Funding

This work was supported by the French Ministry of Higher Education and Research ("Ministère de l'Enseignement Supérieur et de la Recherche"), Inserm (Institut National de la Santé et de la Recherche Médicale; UMR1071), INRAE (Institut National de Recherche en Agriculture, Alimentation et Environnement; USC 1382), the ANR (French National Research Agency) through the program "Future Investments" (I-SITE Clermont, CAP 20-25; Projects RUNINGUT, EXOCROHN and HAPPYCROHN to Hang Nguyen) and for funding the project ANR PRC AAPG2021_RESTOGUT (to Hang Nguyen) and the national program "Microbiote" Inserm (to N. Barnich).

References

[1] Patel SG, Karlitz JJ, Yen T, et al. The rising tide of early-onset colorectal cancer: a comprehensive review of epidemiology, clinical features, biology, risk factors, prevention, and early detection. Lancet Gastroenterol Hepatol. 2022;7(3):262–274. doi: 10.1016/S2468-1253(21)00426-X

[2] Lucas C, Barnich N, Nguyen NH. Microbiota, inflammation and colorectal cancer. Int J Mol Sci. 2017;18(6):E1310. doi: 10.3390/ijms18061310

[3] Janney A, Powrie F, Mann EH. Host–microbiota maladaptation in colorectal cancer. Nature. 2020;585(7826):509–517. doi: 10.1038/s41586-020-2729-3

[4] Arthur JC, Perez-Chanona E, Mühlbauer M, et al. Intestinal inflammation targets cancer-inducing activity of the microbiota. Science. 2012;338(6103):120–123. doi: 10.1126/science.1224820

[5] Dejea CM, Fathi P, Craig JM, et al. Patients with familial adenomatous polyposis harbor colonic biofilms containing tumorigenic bacteria. Science. 2018;359(6375):592–597. doi: 10.1126/science.aah3648

[6] Iyadorai T, Mariappan V, Vellasamy KM, et al. Prevalence and association of pks+ Escherichia coli with colorectal cancer in patients at the University Malaya Medical Centre, Malaysia. PLoS One. 2020;15(1):e0228217. doi: 10.1371/journal.pone.0228217

[7] Buc E, Dubois D, Sauvanet P, et al. High prevalence of mucosa-associated E. coli producing cyclomodulin and genotoxin in colon cancer. PLoS One. 2013;8(2):e56964. doi: 10.1371/journal.pone.0056964

[8] Pleguezuelos-Manzano C, Puschhof J, Rosendahl Huber A, et al. Mutational signature in colorectal cancer caused by genotoxic pks + E. coli. Nature. 2020;580(7802):269–273. doi: 10.1038/s41586-020-2080-8

[9] Lucas C, Salesse L, Hoang MHT, et al. Autophagy of intestinal epithelial cells inhibits colorectal carcinogenesis induced by colibactin-producing Escherichia coli in ApcMin/+ Mice. Gastroenterology. 2020;158(5):1373–1388. doi: 10.1053/j.gastro.2019.12.026

[10] Larabi A, Barnich N, Nguyen HTT. New insights into the interplay between autophagy, gut microbiota and inflammatory responses in IBD. Autophagy. 2020;16(1):38–51. doi: 10.1080/15548627.2019.1635384

[11] Nguyen HTT, Lapaquette P, Bringer M-A, et al. Autophagy and Crohn's disease. J Innate Immun. 2013;5(5):434–443. doi: 10.1159/000345129

[12] Lapaquette P, Nguyen HTT, Faure M. L'autophagie garante de l'immunité et de l'inflammation. Med Sci (Paris). 2017;33(3):305–311. doi: 10.1051/medsci/20173303018

[13] Salesse L, Lucas C, Hoang MHT, et al. Colibactin-producing Escherichia coli induce the formation of invasive carcinomas in A chronic inflammation-associated mouse model. Cancers (Basel). 2021;13(9):2060. doi: 10.3390/cancers13092060

[14] Weinberg F, Ramnath N, Nagrath D. Reactive oxygen species in the tumor microenvironment: an overview. Cancers (Basel). 2019;11(8):E1191. doi: 10.3390/cancers11081191

[15] Lopès A, Billard E, Casse AH, et al. Colibactin-positive Escherichia coli induce a procarcinogenic immune environment leading to immunotherapy resistance in colorectal cancer. Int J Cancer. 2020;146(11):3147–3159. doi: 10.1002/ijc.32920

[16] Guo L, Wang C, Qiu X, et al. Colorectal cancer immune infiltrates: significance in patient prognosis and immunotherapeutic efficacy. Front Immunol. 2020;11:1052. doi: 10.3389/fimmu.2020.01052

[17] Klionsky DJ, Abdel-Aziz AK, Abdelfatah S, et al. Guidelines for the use and interpretation of assays for monitoring autophagy (4th edition). Autophagy. 2021;17(1):1–382. doi: 10.1080/15548627.2020.1797280

[18] Nguyen HTT, Dalmasso G, Müller S, et al. Crohn's disease–associated adherent invasive Escherichia colI modulate levels of microrna in intestinal epithelial cells to reduce autophagy. Gastroenterology. 2014;146(2):508–519. doi: 10.1053/j.gastro.2013.10.021

[19] Bretin A, Carrière J, Dalmasso G, et al. Activation of the EIF2AK4-EIF2A/eIF2α-ATF4 pathway triggers autophagy response to Crohn disease-associated adherent-invasive Escherichia coli infection. Autophagy. 2016;12(5):770–783. doi: 10.1080/15548627.2016.1156823

[20] Larabi A, Dalmasso G, Delmas J, et al. Exosomes transfer miRnas from cell-to-cell to inhibit autophagy during infection with Crohn's disease-associated adherent-invasive E. coli. Gut Microbes. 2020;11(6):1677–1694. doi: 10.1080/19490976.2020.1771985

[21] Bretin A, Lucas C, Larabi A, et al. AIEC infection triggers modification of gut microbiota composition in genetically predisposed mice, contributing to intestinal inflammation. Sci Rep. 2018;8(1):12301. doi: 10.1038/s41598-018-30055-y

[22] Dalmasso G, Nguyen HTT, Faïs T, et al. Crohn's disease-associated adherent-invasive Escherichia coli manipulate host autophagy by impairing sumoylation. Cells. 2019;8(1):35. doi: 10.3390/cells8010035

[23] Dalmasso G, Nguyen HTT, Faïs T, et al. Yersiniabactin siderophore of Crohn's disease-associated adherent-invasive Escherichia coli is involved in autophagy activation in host cells. Int J Mol Sci. 2021;22(7):3512. doi: 10.3390/ijms22073512

[24] Zheng W, Wu J, Peng Y, et al. Tumor-associated neutrophils in colorectal cancer development, progression and immunotherapy. Cancers (Basel). 2022;14(19):4755. doi: 10.3390/cancers14194755

[25] Gerada C, Ryan KM. Autophagy, the innate immune response and cancer. Mol Oncol. 2020;14(9):1913–1929. doi: 10.1002/1878-0261.12774

[26] Long AG, Lundsmith ET, Hamilton KE. Inflammation and colorectal cancer. Curr Colorectal Cancer Rep. 2017;13(4):341–351. doi: 10.1007/s11888-017-0373-6

[27] Rébé C, Ghiringhelli F. Interleukin-1β and cancer. Cancers (Basel). 2020;12(7):1791. doi: 10.3390/cancers12071791

[28] Hai Ping P, Feng Bo T, Li L, et al. IL-1β/NF-kb signaling promotes colorectal cancer cell growth through miR-181a/PTEN axis. Arch Biochem Biophys. 2016;604:20–26. doi: 10.1016/j.abb.2016.06.001

[29] Kaler P, Augenlicht L, Klampfer L. Macrophage-derived IL-1β stimulates Wnt signaling and growth of colon cancer cells: a crosstalk interrupted by vitamin D3. Oncogene. 2009;28(44):3892–3902. doi: 10.1038/onc.2009.247

[30] Abais JM, Xia M, Zhang Y, et al. Redox regulation of NLRP3 Inflammasomes: ROS as trigger or effector? Antioxid Redox Signal. 2015;22(13):1111–1129. doi: 10.1089/ars.2014.5994

[31] Zheng D, Liwinski T, Elinav E. Inflammasome activation and regulation: toward a better understanding of complex mechanisms. Cell Discov. 2020;6(1):36. doi: 10.1038/s41421-020-0167-x

[32] Iwaniuk A, Jablonska E. Neutrophils in health and disease: from receptor sensing to inflammasome activation. IJMS. 2023;24(7):6340. doi: 10.3390/ijms24076340

[33] SenGupta S, Hein LE, Parent CA. The recruitment of neutrophils to the tumor microenvironment is regulated by multiple mediators. Front Immunol. 2021;12:734188. doi: 10.3389/fimmu.2021.734188

[34] Wu S, Rhee K-J, Albesiano E, et al. A human colonic commensal promotes colon tumorigenesis via activation of T helper type 17 T cell responses. Nat Med. 2009;15(9):1016–1022. doi: 10.1038/nm.2015

[35] DeStefano SC, White JR, Chung L, et al. Bacterial-driven inflammation and mutant BRAF expression combine to promote murine colon tumorigenesis that is sensitive to immune checkpoint therapy. Cancer Discovery. 2021;11(7):1792–1807. doi: 10.1158/2159-8290.CD-20-0770

[36] Zhang X, Yu D, Wu D, et al. Tissue-resident lachnospiraceae family bacteria protect against colorectal carcinogenesis by promoting tumor immune surveillance. Cell Host Microbe. 2023;31(3):418–432.e8. doi: 10.1016/j.chom.2023.01.013

[37] Gammoh N. The multifaceted functions of ATG16L1 in autophagy and related processes. J Cell Sci. 2020;133(20):jcs249227. doi: 10.1242/jcs.249227

[38] Adolph TE, Tomczak MF, Niederreiter L, et al. Paneth cells as a site of origin for intestinal inflammation. Nature. 2013;503(7475):272–276. doi: 10.1038/nature12599

[39] Clausen BE, Burkhardt C, Reith W, et al. Conditional gene targeting in macrophages and granulocytes using LysMcre mice. Transgenic Res. 1999;8(4):265–277. doi: 10.1023/A:1008942828960